



UNIVERSITÀ DI PARMA

DIPARTIMENTO DI SCIENZE MATEMATICHE, FISICHE E INFORMATICHE
Corso di Laurea Triennale in Informatica

Deep Reinforcement Learning per la Manipolazione con Fisica di Oggetti in Ambienti Ingombri Bidimensionali

*Deep Reinforcement Learning for 2D Physics-Based Object
Manipulation in Clutter*

CANDIDATO:
Luca Renna

RELATORE:
Prof. Francesco Morandin

CORRELATORE:
Prof. Matteo Leonetti

Sommario

Il Deep Reinforcement Learning (DRL) è un ambito di ricerca in rapida evoluzione con radici nella ricerca operativa e nella psicologia comportamentale, e con potenziali applicazioni che si estendono in vari domini, compreso quello della robotica. Questa tesi delinea le basi per il Reinforcement Learning (RL) moderno, partendo dall'impostazione matematica data dai Markov decision processes, la Markov property, goals e rewards, interazioni agente-ambiente e policies. Spieghiamo i principali tipi di algoritmi comunemente utilizzati nell'RL, inclusi i metodi value-based, policy gradient, e actor-critic, con particolare attenzione agli algoritmi DQN, A2C e PPO. Successivamente, forniamo una breve rassegna della letteratura corrente su alcuni dei framework di uso comune per lo sviluppo di algoritmi e ambienti di RL. In seguito, presentiamo il Bidimensional Gripper Environment (BGE), un simulatore virtuale basato sul motore fisico Pymunk, che abbiamo sviluppato per la analisi della manipolazione bidimensionale di oggetti con vista dall'alto. La sezione della metodologia spiega come la nostra interazione agente-ambiente si possa inquadrare come un Markov decision process, in modo tale da poter applicare i nostri algoritmi di RL. Dopodichè elenchiamo varie strategie di formulazione dei goal, incluse il reward shaping e il curriculum learning. Impieghiamo anche numerosi passaggi di pre-processing delle osservazioni per ridurre il carico computazionale necessario. Nella fase sperimentale, affrontiamo una serie di scenari di difficoltà crescente. Iniziamo con uno scenario statico semplice, per poi aumentare gradualmente il livello di stocasticità. Ogni volta che gli agenti mostrano difficoltà nell'apprendimento, controbilanciamo aumentando il grado di reward shaping e curriculum learning. Questi esperimenti mostrano le forti limitazioni e le insidie degli algoritmi model-free in ambienti dinamici. In conclusione, presentiamo un riepilogo dei risultati accompagnati da alcune osservazioni. Quindi deliniamo alcuni possibili sviluppi futuri per migliorare sia la nostra metodologia sia per un possibile ampliamento a sistemi in ambiente reale.

Abstract

Deep Reinforcement Learning (DRL) is a quickly evolving research field rooted in operations research and behavioural psychology, with potential applications extending across various domains, including robotics. This thesis delineates the background of modern Reinforcement Learning (RL), starting with the framework constituted by the Markov decision processes, Markov properties, goals and rewards, agent-environment interactions, and policies. We explain the main types of algorithms commonly used in RL, including value-based, policy gradient, and actor-critic methods, with a special emphasis on DQN, A2C and PPO. We then give a short literature review on some widely adopted frameworks for implementing RL algorithms and environments. Subsequently, we present Bidimensional Gripper Environment (BGE), a virtual simulator based on the Pymunk physics engine we developed to analyse top-down bidimensional object manipulation. The methodology section frames our agent-environment interaction as a Markov decision process, such that we can apply our RL algorithms. We list various goal formulation strategies, including reward shaping and curriculum learning. We also employ different steps of observation preprocessing to reduce the computational workload required. In the experimental phase, we run through a series of scenarios of increasing difficulty. We start with a simple static scenario and then gradually increase the amount of stochasticity. Whenever the agents show difficulty in learning, we counteract by increasing the degree of reward shaping and curriculum learning. These experiments demonstrate the substantial limitations and pitfalls of model-free algorithms under changing dynamics. In conclusion, we present a summary of our findings and remarks. We then outline potential future work to improve our methodology and possibly expand to real-world systems.

Contents

1	Introduction	1
1.1	Brief History of Reinforcement Learning	2
1.2	Motivation and Objectives	5
1.3	Scope and Limitations	5
1.4	Thesis Outline	6
2	Background	7
2.1	Reinforcement Learning Framework	7
2.1.1	Markov Decision Process	8
2.1.2	Markov Property	9
2.1.3	Goals and Rewards	10
2.1.4	Return	10
2.1.5	Episodic and Continuing tasks	11
2.1.6	Agent and Environment Interaction	11
2.1.7	Full and Partial Observability	12
2.1.8	Action Spaces	12
2.1.9	Policies	12
2.2	Value Functions	13
2.2.1	Bellman Equations	14
2.2.2	Bellman Optimality Equations	14
2.2.3	Optimal Value Functions and Optimal Policies	15
2.2.4	Advantage Function	16
2.2.5	Exploration and Exploitation Trade-off	17
2.3	Model-Free and Model-Based	17
3	Reinforcement Learning Algorithms	19
3.1	Value-based Methods	20
3.1.1	Policy Iteration	20
3.1.2	Generalised Policy Iteration	21
3.1.3	On-policy and Off-policy Methods	22
3.1.4	Monte Carlo Methods	23

3.1.5	Temporal-Difference Methods	24
3.1.6	Q-Learning	25
3.2	Value-based Methods with Approximation	25
3.2.1	Stochastic-gradient Methods	27
3.2.2	Semi-gradient Methods	27
3.2.3	Function Approximation with Off-policy Methods	28
3.2.4	Deep Q-Learning	29
3.3	Policy Gradient Methods	32
3.3.1	The Policy Gradient Theorem	32
3.3.2	REINFORCE	33
3.3.3	REINFORCE with Baseline	34
3.4	Actor-Critic Methods	35
3.4.1	Advantage Actor-Critic	36
3.4.2	Proximal Policy Optimisation (Clip)	37
4	Related Work	41
4.1	Algorithms	41
4.2	Environments	42
4.3	Physics Object Manipulation	43
5	Methodology	45
5.1	Environment	45
5.1.1	Agent-environment Interaction as an MDP	46
5.2	Observation Preprocessing	47
5.3	Goal Formulation and Evaluation Metrics	48
5.3.1	Binary Sparse Rewards	49
5.3.2	Reward Shaping	49
5.3.3	Curriculum Learning	51
5.3.4	Domain Randomisation	51
5.3.5	Evaluation Metrics	51
5.4	Agent Architecture	52
5.4.1	Deep Q-Network Architecture	53
5.4.2	Actor-Critic Architecture	54
5.5	Training and Evaluation	55
5.5.1	Algorithms and Environment Parameters	56
6	Experiments	59
6.1	Experiment I	60
6.1.1	Results	62
6.2	Experiment II	62
6.2.1	Results	64

6.3	Experiment III	64
6.3.1	Results	66
6.4	Experiment IV	66
6.4.1	Results	68
6.5	Experiment V	68
6.5.1	Results	70
6.6	Experiment VI: Extended Training	70
6.6.1	Results	73
7	Conclusion and Future Work	75
7.1	Results Discussion	75
7.2	Future Work	76
7.3	Conclusions	76
	Bibliography	79
	List of Figures	87
	List of Algorithms	89
	List of Tables	91
	List of Acronyms	93
	A Summary of Notation	I

Acknowledgements

I wish to extend my heartfelt gratitude to my supervisor, Professor Matteo Leonetti, for his guidance and support throughout this project. The opportunity to work at the King's College London Centre for Doctoral Research (CDT) has been invaluable, and his passion, expertise, and constructive feedback have inspired me to continue my studies in this field. Additionally, I am grateful to Professor Francesco Morandin, my home supervisor at the University of Parma, for his invaluable insight and contribution. My appreciation extends to all the members of the CDT. Their assistance and camaraderie made my journey enjoyable and enriching. In particular, I would like to thank Dr. Gabriele La Malfa, whose words of encouragement and insightful discussions were a constant source of motivation, and Dr. Nathan Schneider Gavenski for his invaluable advice regarding my experiments and methodology. I express my gratitude to the Computer Science and Erasmus Department staff at the University of Parma, especially to Professor Roberto Bagnara and Dr. Alessandro Bernazzoli for making the exchange a reality. On a personal note, I am eternally grateful to my friends and family. A special thank you to my parents, Claudia and Antonio, whose unwavering encouragement and support have been my pillars of strength. Lastly, I wish to acknowledge the immense contribution of the developers and contributors behind the open-source tools and libraries utilized in my thesis. Without their dedication and expertise, this project would not have come to fruition. Please note that this research benefits from the High-Performance Computing facility of the University of Parma, Italy.

Chapter 1

Introduction

Reinforcement Learning (RL) is an approach deeply inspired by how humans acquire knowledge. We engage with our environment, assess the outcomes of our actions, and learn from the feedback we receive. This learning method allows us to adapt our behaviours to attain specific objectives, whether playing a musical instrument, learning to drive, playing a game like chess, or even acquiring a new language.

In Computer Science, RL emerges as a computational paradigm emphasising learning through interaction. Its primary goal is to maximise the expected return of a numerical reward signal, positioning itself as a contrast to the traditional Supervised Learning (SL) methods. Unlike SL, which necessitates labelled datasets comprising observations and corresponding ground truths, RL does not rely on such explicit supervision. This distinction is pivotal, as constructing large labelled datasets can be labour-intensive, inefficient, and challenging, especially when it is difficult to discern a definitive ground truth.

RL methods dispense with the need for ground truths, empowering models to learn through self-play, trial-and-error, and direct interaction with their environment. Data is procured autonomously, with outcomes, such as success or failure, attributed to this data post-collection.

Deep Learning (DL) offers a solution to navigate the unpredictability of the real world. By training a highly parametrised model, like a deep neural network, Deep Reinforcement Learning (DRL) can efficiently handle vast state spaces where traditional RL methods fall short. A typical configuration includes a convolutional layer followed by a specialised, fully connected layer, where the entire architecture is trained end-to-end. In this setup, the convolutional layer can be perceived as a "visual cortex" that autonomously sifts through observations to identify pertinent features. These features are subsequently evaluated by the fully connected layer, functioning akin to a

"motor cortex" to determine the most appropriate action for the agent.

While RL lays the mathematical and algorithmic groundwork, deep models supplement it with powerful representations. Together, they enable scaling to real-world systems.

1.1 Brief History of Reinforcement Learning

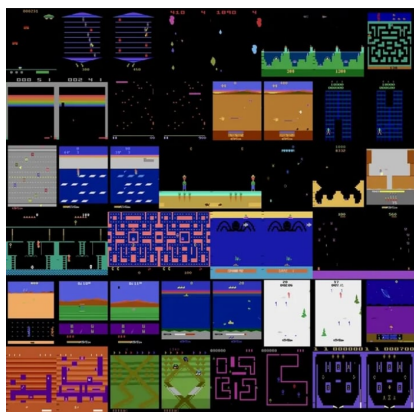


Figure 1.1: Frames of different Atari games. Source: DeepMind (2020b).



Figure 1.2: International go champion Lee Sedol plays against AlphaGo in a five-game match. Source: DeepMind (2020a).

As recognised today, modern RL emerged in the late 1980s. It synthesised principles from optimal control theory, trial-and-error learning, temporal-difference techniques, and other fields such as neuroscience, animal psychology and operation research. Most of its mathematical foundation, including notations, draws from optimal control and dynamic programming, notably, the Bellman Equations (Sutton & Barto, 2018).

Recent advancements highlight the potent combination of Reinforcement Learning and Deep Learning, offering vast applications across various domains. Traditional tabular methods grapple with the curse of dimensionality in expansive state spaces, leading to storage challenges and extensive training requirements. To address these constraints, function approximation methods have been introduced. These methods aim to generalise across similar states. However, linear function approximators often fall short in complex tasks, where determining a relevant subset of features is non-trivial ().

Nonlinear function approximators, such as Artificial Neural Networks (AANs), offer a solution. These networks are designed to automatically

discern and craft features suitable for specific tasks, reducing the reliance on manual feature engineering. A significant advancement in this area has been the integration of Deep Convolutional Neural Networks (CNNs). These networks have showcased their capability in end-to-end training, using raw images as state representations, leading to notable breakthroughs in the field (). Analysis of convergence properties of reinforcement learning algorithms using function approximation is complicated. Results for TD learning have been progressively strengthened for the case of linear function approximators, but several examples of divergence have been presented for nonlinear functions ().

Recent successes in the field of DRL demonstrate the potential of these techniques. Despite the existing gap between theoretical guarantees and empirical performance, real-world applications of DRL have repeatedly yielded results surpassing human expertise. An early testament to this was Tesauro’s TD-Gammon 0.0 (), a backgammon-playing program that used a multi-layer AAN for Temporal Difference (TD)(lambda) function approximation (Sutton, 1988). Starting only with a raw representation of the board state and minimal game rules, this program reached master-level performance through self-play. However, while later versions of TD-Gammon improved play using handcrafted features, initial efforts to replicate this success in more complex games like chess, Go, and checkers fell short, leading to the widespread belief that TD-Gammon’s nonlinear approximation strategy might be uniquely suited for backgammon (Pollack & Blair, 1996).

This scepticism was soon dispelled by a team of researchers at DeepMind. Through their research, they demonstrated that deep convolutional AANs could be seamlessly integrated into RL to autonomously design features from raw visual inputs of the environment state (). Their pioneering agent, using a Deep Q-Network (DQN), achieved a high level of play across a diverse set of 49 Atari games within the Arcade Learning Environment (ALE) (Bellemare et al., 2013), all without any prior knowledge of game rules. Remarkably, a uniform network architecture, algorithm, and set of hyperparameters were employed across these games. This accomplishment showcased unprecedented generalisation abilities and marked a significant departure from the prevailing reliance on meticulously handcrafted features in DRL.

Building on their earlier achievements in DRL, DeepMind unveiled their groundbreaking AlphaGo program (Silver et al., 2016). This software not only managed to defeat world champions at Go—a feat once considered years, if not decades, away from realisation—but also illustrated once again the transformative potential of merging DL and RL. AlphaGo was trained using Deep Neural Networks (DNNs) with a combination of initial SL on a large

dataset of expert human moves, followed by RL via self-play on simulations of Go. Central to its design was a modified Monte Carlo Tree Search (MCTS), guided by both policy and value functions, with CNNs employed for function approximation. One year later, the next iteration of the program, AlphaGo Zero (Silver et al., 2017), outperformed its predecessor. Impressively, it attained this without any human-derived data or input, relying solely on the game’s basic rules. Its architecture was not only simpler by doing away with SL and using a quicker MCTS but also more potent, achieving superhuman performance exclusively through self-play. The evolution continued with AlphaZero, which generalised the original program to master Chess and Shogi (Silver et al., 2018). Finally, the advent of MuZero (Schrittwieser et al., 2020) marked a paradigm shift. Unlike its precursors, which needed to be provided with predefined models of their respective games, MuZero needed no prior knowledge and used DRL to learn and refine its internal model to simulate the environment dynamics, which would query to plan ahead.

The innovative streak of the AlphaGo series did not limit itself to games but underscored the versatility of DRL in various other scientific domains. AlphaFold, for instance, addressed a long-standing challenge in modern biology: it efficiently predicted the 3D structures of nearly all known proteins, marking a significant milestone (). AlphaTensor achieved a breakthrough in computational mathematics by devising a 4x4 matrix multiplication technique that surpassed Strassen’s algorithm—a standard that had held its ground for over half a century (Fawzi et al., 2022). Furthermore, the foundational principles of the AlphaZero algorithm found utility in quantum computing, demonstrating its adaptability to diverse challenges (Dalgaard et al., 2020).

Recently, there has been a noticeable shift towards embracing simple yet highly scalable DRL algorithms and architectures, particularly those that can harness enormous parallel computing power (Schulman et al., 2017). A prominent instance of highly distributed RL is seen with OpenAI’s OpenAiFive. OpenAI et al. (2019) explains how they exploited the scalability of Proximal Policy Optimisation (PPO) by training agents on an unprecedented scale using up to 1536 GPUs over a span of 10 months. Similarly, the GPT3-4 series of transformer models represents another remarkable application. These models were also trained using large-scale deployments of PPO on DNN followed by Reinforcement Learning from Human Feedback during the finetuning process, showcasing the versatility and strength of these approaches ().

1.2 Motivation and Objectives

The motivation for this thesis is threefold. First and foremost, it is to provide a general introduction to RL, structured so that the reader should not need any preliminary knowledge of the field. We first give the definitions and background information of traditional RL and describe some classic methods and algorithms. We then expand those methods to the function approximation case, introducing new concepts until the reader has all the necessary knowledge to understand a selection of state-of-the-art algorithms. Second, we want to provide a standardised environment that can be used with those algorithms. One of the critiques against research in the Deep Reinforcement Learning field is the lack of standardisation. Significant efforts have recently been made to standardise algorithm implementations and agent environments. Here, we follow the Gymnasium APIs (Towers et al., 2023) and their best practices to make our environment fully standardised. We follow the Stable Baselines 3 framework (Raffin et al., 2021) for training our agents, and the seeds and hyperparameters are included here for reproducibility. Last, we wish to benchmark and explore some widely adopted model-free DRL algorithms in our environment. Research shows that kinodynamic planning usually works well in physics-based environments. A key issue with some of these classic optimal control open-loop methods is that the computed solution is static and does not adapt to unexpected changes. This poses problems in highly dynamic environments and can be further compounded by the inaccuracies in the physics model used to compute these solutions. The planning is often onerous, so we cannot change it at execution time if we want to remain within the constraints of a real-time system. In our experiments, we use RL methods, which are augmented by DL function approximation to make them suited to learn real-time interaction in systems with large state spaces. Moreover, we also use a raw image representation of the environment to allow a potentially arbitrary number of obstacles to be in the environment without (in theory) needing retraining, provided that the model generalisation capabilities are good enough.

1.3 Scope and Limitations

The scope of this thesis is limited to model-free methods for two primary reasons. First, including model-based approaches would significantly expand the breadth of the thesis, diverging from its introductory purpose. Second, model-based methods are known to be particularly challenging to implement, which would detract from this work’s goal of serving as an approachable

introduction to RL rather than a display of more advanced concepts.

Computational restrictions also bound our experiments. While the studies mentioned in section 1.1 devoted thousands of hours to training their models, we have constrained our training time to a maximum of one day due to sharing computational resources with other groups. Allowing for a longer training duration might have led to better results.

Furthermore, this project remains within the bounds of a simulated environment, sidestepping the exploration of the "sim-to-real gap." Although a potential goal would be to use the robot gripper model trained in a simulation for a real-world application, we have yet to undertake any real-world testing or preliminary studies on transferring our models from the simulator to a real environment.

1.4 Thesis Outline

In chapter 2 on the facing page, we give the mathematical notation and foundational knowledge to understand the RL concepts used in subsequent chapters. The chapter 3 on page 19 provides an overview of both value-based and policy-gradient RL methods, starting with the basic tabular algorithms and leading up to the function approximation case. Here, we give the detailed description of DQN, Advantage Actor-Critic (A2C) and PPO, which we will then use in our experiments. In chapter 2 on the facing page, we give an overview of other standardised environments and frameworks in DRL, along with relevant literature on physics-based object manipulation. The chapter 5 on page 45 describes the Bidimensional Gripper Environment (BGE) environment along with preprocessing steps, our goal formulation and the agent network architecture. In chapter 6 on page 59, we present a series of experiments we run on our environment and their results. In the final chapter 7 on page 75, we conclude with an analysis of our results, and we discuss possible directions for future work.

Chapter 2

Background

This chapter provides a summary of the background and the relevant theoretical foundations of RL utilised in further chapters of this thesis. Initially, we delineate the general framework of RL, introducing the fundamental concept of Markov Decision Process (MDP), which is central to defining interactions in terms of states, actions, and rewards. Subsequently, we articulate goals, rewards, returns, and the differentiation between episodic and continuing tasks. Moreover, we offer a brief overview of the various types of environments encountered in RL and emphasise the significance of policies. The following sections detail the Bellman Equations and Bellman Optimality Equations, utilising their self-consistency property to introduce value functions. Following this, we illustrate the relationship between optimal policies and optimal value function, and we end the section by explaining the central trade-off between exploration and exploitation. We conclude the chapter by distinguishing between model-free and model-based RL approaches, highlighting their respective strengths and weaknesses. The bulk of the definitions and explanations are taken from Sutton and Barto (2018), Francois-Lavet et al. (2018), Achiam (2018), Silver (2015), which the author recommends as additional resources. The thesis does not delve into DL and AANs, which we use here for nonlinear function approximators. Readers interested in DL should consult additional resources such as LeCun et al. (2015) and Goodfellow et al. (2016). The notation used throughout the text is taken from Sutton and Barto (2018) and is made available as appendix A on page I.

2.1 Reinforcement Learning Framework

RL is a computational approach to automating and comprehending decision-making and goal-oriented learning. Its uniqueness stems from its reliance on

direct environment-agent interactions for learning, sidestepping the need for model completeness or explicit supervision. RL leverages Markov Decision Processes (MDPs) to define interactions between the agent and its environment, encompassing states, actions, and rewards. This model provides a concise representation of the Artificial Intelligence problem, including cause-effect relationships, inherent uncertainty, and the presence of an explicit goal. Value functions are fundamental to many RL methods examined in this thesis. Incorporating value functions differentiates RL from evolutionary methods that search the policy space guided by holistic policy evaluations. Another key aspect that makes RL stand out from other machine learning paradigms is that the agent's actions affect subsequent data it receives, making the training datasets time-dependent and based on sequential, non i.i.d data. The decisions also unfold over time, making the rewards delayed.

We use MDPs to frame the problem of learning from interaction to achieve a goal. In this setup, the "learner" or "decision-maker" is known as the agent. Everything that the agent interacts with outside of itself is called the environment. The dividing line between the agent and its environment is not always a physical barrier, like the body of a robot or an animal. The rule of thumb we use is that anything the agent cannot change at will is considered part of the environment, regardless of whether the agent has partial or absolute knowledge of it. Thus, the agent-environment boundary marks the edge of the agent's control, not what it knows. In this ongoing process, the agent chooses actions, and the environment reacts, creating new situations for the agent. The environment also offers rewards—specific numerical values—that the agent tries to increase over time through its chosen actions.

2.1.1 Markov Decision Process

MDPs are a classic formalisation of sequential decision making, where actions influence immediate rewards, subsequent situations, or states, and through those future rewards. Thus, MDPs involve delayed reward and the need to trade off immediate and delayed reward. We model the environment in which the agent acts as an MDP:

Definition 2.1.1 (Markov Decision Process). A *Markov Decision Process (MDP)* is defined by a 4-tuple (S, A, p, r) where:

- S is a finite set of states.
- A is a finite set of actions.

- $p : \mathcal{S} \times \mathcal{R} \times \mathcal{S} \times \mathcal{A} \rightarrow [0, 1]$ defines the state transition probability such that $p(s', r | s, a)$ is the probability of transitioning to state s' from state s with reward r by taking action a .
- $r : \mathcal{S} \times \mathcal{A} \times \mathcal{S} \rightarrow \mathbb{R}$ is the reward function where $r(s, a, s')$ gives the immediate reward for taking action a from state s and transitioning to state s' .

In a finite MDP, the set of states, actions, and rewards (\mathcal{S} , \mathcal{A} , and \mathcal{R}) all have a finite number of elements. In this case, the random variables R_t and S_t have well-defined discrete probability distributions dependent only on the preceding state and action. That is, for particular values of these random variables, $s' \in \mathcal{S}$ and $r \in \mathcal{R}$, there is a probability of those values occurring at time t , given particular values of the preceding state and action:

$$p(s', r | s, a) \doteq \Pr\{S_t = s', R_t = r \mid S_{t-1} = s, A_{t-1} = a\}, \quad (2.1)$$

for all $s', s \in \mathcal{S}, r \in \mathcal{R}$ and $a \in \mathcal{A}(s)$. The function p defines the dynamics of the MDP. The dynamics function p is an ordinary deterministic function of four arguments which specifies a probability distribution for each choice of s and a , that is, that

$$\sum_{s' \in \mathcal{S}} \sum_{r \in \mathcal{R}} p(s', r | s, a) = 1, \text{ for all } s \in \mathcal{S}, a \in \mathcal{A}(s).$$

Alternatively, we can also define $r(s, a)$ as a two-argument function that gives the expected rewards for a state-action pair:

$$r(s, a) \doteq \mathbb{E}[R_t \mid S_{t-1} = s, A_{t-1} = a] = \sum_{r \in \mathcal{R}} r \sum_{s' \in \mathcal{S}} p(s', r | s, a). \quad (2.2)$$

From now on, we assume that the environment is an MDP and the symbols $s, s' \in \mathcal{S}, a \in \mathcal{A}(s), r \in \mathcal{R}$ and $p(s', r | s, a)$ gives the environment dynamics.

2.1.2 Markov Property

Definition 2.1.2 (Markov Property). A state S_t is *Markov* if and only if

$$\Pr\{S_{t+1} \mid S_t = s\} = \Pr\{S_{t+1} \mid S_0 = s_0, \dots, S_t = s\}.$$

A key property of an MDP is that transitions only depend on the most recent state and action and no prior history. That is, the probability of each possible value for S_t and R_t depends on the immediately preceding state S_{t-1} and action A_{t-1} and, given them, not on all earlier states and actions. The state must include information about all aspects of the past agent–environment interactions that make a difference in the future. If it does, the state is said to have the *Markov property*.

2.1.3 Goals and Rewards

The reward signal defines the goal of a RL problem. The environment sends the agent a number called the reward on each timestep. The agent's sole objective is to maximise the cumulative reward, the total future reward it receives over the long run. RL is based on the *reward hypothesis* in definition 2.1.3, meaning that the maximisation of expected cumulative reward can describe all goals.

Definition 2.1.3 (The Reward Hypothesis). All of what we mean by goals and purposes can be well thought of as the maximisation of the expected value of the cumulative sum of a received scalar signal (called reward) (Sutton & Barto, 2018, p. 53).

2.1.4 Return

As we said in section 2.1.3, the agent's goal in RL is to maximise the cumulative reward in the long run, namely the *expected return*. We define the return G_t (also known as *reward-to-go*) as some specific function of the reward sequence:

Definition 2.1.4 (Return). The return G_t is the total discounted reward from timestep t .

$$G_t \doteq R_{t+1} + \gamma R_{t+2} + \gamma^2 R_{t+3} + \dots = \sum_{k=0}^{\infty} \gamma^k R_{t+k+1},$$

where γ is a parameter $0 \leq \gamma \leq 1$, called the *discount rate*.

Returns at successive timesteps are related to each other in a way that is important for the theory and algorithms of RL:

$$\begin{aligned} G_t &\doteq R_{t+1} + \gamma R_{t+2} + \gamma^2 R_{t+3} + \gamma^3 R_{t+4} + \dots \\ &= R_{t+1} + \gamma G_{t+1}, \end{aligned} \tag{2.3}$$

To ensure the infinite sum in definition 2.1.4 yields a finite value, we permit an undiscounted return (where $\gamma = 1$) exclusively in tasks where all sequences terminate. We use discounting on the return for several rationales, including making returns more mathematically convenient, avoiding infinite returns in cyclic Markov processes, accounting for future uncertainties and regulating the emphasis between immediate and delayed rewards. We can adjust γ to place more or less value on immediate rewards above delayed rewards, where γ close to 0 leads to a "myopic" evaluation and γ close to 1 leads to a "far-sighted" evaluation.

2.1.5 Episodic and Continuing tasks

When the agent-environment naturally breaks into distinct subsequences, we refer to the task at hand as an *episodic task*. Each episode ends in a special state called the *terminal state*, followed by a reset to a standard starting state or a sample from a standard distribution of starting states. Every episode begins independently of how the previous one ended. Conversely, a *continuing task* is characterised by the agent-environment interaction going on continually without limit. The return formulation shown in definition 2.1.4 holds for both episodic and continuing tasks. We will use notation and algorithms assuming an episodic task in this and subsequent chapters. However, most concepts can be easily generalised to accommodate continuing tasks.

2.1.6 Agent and Environment Interaction

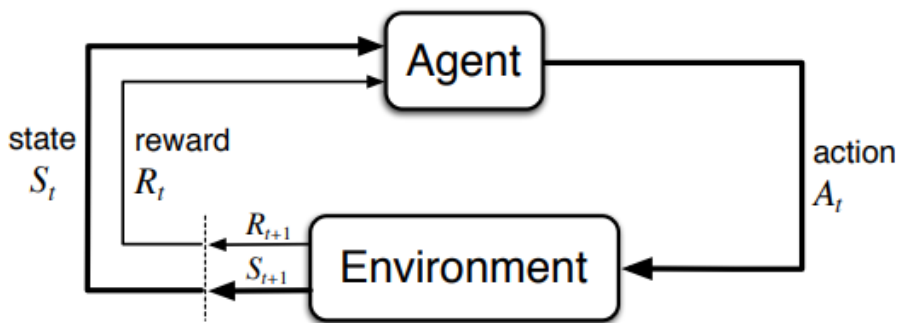


Figure 2.1: The agent-environment interaction in a Markov Decision Process. Source: Sutton and Barto (2018, p. 48).

At each timestep, t , the agent receives some representation of the environment’s state $S_t \in \mathcal{S}$ and, on that basis, selects an action, $A_t \in \mathcal{A}(s)$. One timestep later, the agent receives a numerical reward, $R_{t+1} \in \mathcal{R} \subset \mathbb{R}$, and finds itself in a new state, S_{t+1} . The MDP and agent together thereby give rise to a sequence or *trajectory* τ that begins as follows:

$$\tau = S_0, A_0, R_1, S_1, A_1, R_2, S_2, A_2, R_3, \dots$$

Where the very first state of the world S_0 is randomly sampled from the start-state distribution μ_0 , namely $S_0 \sim \mu_0(\cdot)$. We call a complete trajectory from a start state to a final state an *episode* or *rollout*.

2.1.7 Full and Partial Observability

We defined S_t as the environment’s state representation, meaning whatever data the environment uses to pick the following observation and reward. However, in many cases, potentially essential aspects of the environment’s state are not directly observable or may contain irrelevant information. In that case, the environment emits not its states but observations O_t that provide only partial information about it. When the environment emits complete states $O_t = S_t$, we call the problem *fully observable* and model it using an MDP. Otherwise, it is *partially observable*, and we use a Partially Observable Markov Decision Process. Here, we always assume the case where we have full observability, but parametrised function approximation in section 3.2 on page 25 can be extended to partially observable environments with no changes. If a state variable is not observable, the parametrisation can be chosen so that the approximate value does not depend on that state variable.

2.1.8 Action Spaces

Different environments permit various types of actions, with the collective set of all legal actions in a given environment being known as the *action space*. Environments such as Atari and Go possess *discrete action spaces*, restricting the agent to a finite set of potential moves. In contrast, scenarios where, for example, the agent manages a robot in a physical realm have *continuous action spaces*, where actions are articulated as real-valued vectors. This differentiation between discrete and continuous action spaces is essential to the methods applied in DRL. Some families of algorithms can only be directly applied to a specific type of action space and would have to be substantially reworked for the other. In the scope of this thesis, the emphasis will be placed on environments characterised by discrete action spaces.

2.1.9 Policies

A policy is a rule used by an agent to decide what actions to take, determining the *behaviour* of an agent at a given time. More formally, a policy is a mapping from states to probabilities of selecting each possible action. If the agent follows policy π at time t , then $\pi(a|s)$ is the probability that $A_t = a$ if $S_t = s$.

Definition 2.1.5 (Policy). A *policy* π is a distribution of states over actions,

$$\pi(a|s) \doteq \Pr\{A_t = a \mid S_t = s\}$$

and gives the probability of taking action a when in state s (also denoted by $a \sim \pi(\cdot|s)$)

We denote the policy by $a = \pi(s)$ when the policy is deterministic. Otherwise, it is assumed to be stochastic. RL methods specify how the agent’s policy changes due to its experience. In the context of DRL, it is standard to work with *parametrised policies*, which are policies whose outputs are computable functions that depend on a set of parameters. These parameters can depend, for example, on a neural network’s weights and biases, which can be fine-tuned to modify the agent’s behaviour through some optimisation algorithm. Within DRL, the prevalent types of stochastic policies are categorical policies and diagonal Gaussian policies. Categorical policies can be used in discrete action spaces, while diagonal Gaussian policies are used in continuous action spaces. Two fundamental computations are key to the utilisation and training of stochastic policies: the sampling of actions from the policy and computing log-likelihoods of specific actions represented as $\log \pi_\theta(a|s)$. A more detailed discussion on parametrised policies will be presented in section 3.3 on page 32.

2.2 Value Functions

Value functions of states or state-action pairs are functions that serve to estimate the expected return for an agent when in a given state or state-action pair and operating under a specific policy forever after. Informally, a state-value function represents the total reward an agent expects to accumulate over time, starting from a particular state and following a policy. Rewards indicate the immediate desirability of states, whereas values convey long-term desirability, factoring in the potential subsequent states and the associated rewards. In the decision-making process, the objective is to choose actions that lead to states with the highest value rather than the highest immediate reward. Central to nearly all RL algorithms is a method for efficiently estimating values.

Definition 2.2.1 (State-value function). The *state-value function* $v_\pi(s)$ of a state s under policy π is the expected return when starting from state s and then following π thereafter.

$$v_\pi(s) \doteq \mathbb{E}_\pi [G_t \mid S_t = s]$$

Definition 2.2.2 (Action-value function). The *action-value function* $q_\pi(s, a)$ of taking action a in a state s under a policy π is the expected return when

starting from state s , taking action a , and thereafter following policy π .

$$q_\pi(s, a) \doteq \mathbb{E}_\pi [G_t \mid S_t = s, A_t = a]$$

2.2.1 Bellman Equations

All four value functions obey special self-consistency equations known as the Bellman equations and are a fundamental property of value function. These equations express a relationship between the state's value and its successor states' values.

The Bellman Equation for v_π is:

$$\begin{aligned} v_\pi(s) &\doteq \mathbb{E}_\pi [G_t \mid S_t = s] \\ &= \sum_a \pi(a|s) \sum_{s',r} p(s', r \mid s, a) [r + \gamma v_\pi(s')], \end{aligned} \quad (2.4)$$

and the Bellman Equation for q_π is given by:

$$\begin{aligned} q_\pi(s, a) &\doteq \mathbb{E}_\pi [G_t \mid S_t = s, A_t = a] \\ &= \sum_{s',r} p(s', r \mid s, a) \left[r + \gamma \sum_{a'} \pi(a'|s') q_\pi(s', a') \right]. \end{aligned} \quad (2.5)$$

2.2.2 Bellman Optimality Equations

The Bellman optimality equation is a system of equations, each corresponding to an individual state. Suppose the dynamics π of the environment are known. In that case, one can theoretically solve this equation system for v_* using any one of a variety of methods for solving systems of nonlinear equations, such as Dynamic Programming (DP). Explicitly solving the equation provides one route to finding the optimal policy and solving the RL problem. However, this solution is rarely useful as it is akin to an exhaustive search. This solution rests on three assumptions that are rarely true in practice: (1) the dynamics of the environment are accurately known (2) computational resources are sufficient to complete the calculation and (3) the states have the Markov property. In most tasks, a combination of these assumptions is violated. Hence, in RL, one must settle for approximate solutions. Many RL methods can be clearly understood as approximatively solving the Bellman optimality equation using actual sampled transitions instead of knowledge of expected transitions. This online nature of RL makes it possible to approximate optimal policies in ways that put more effort into

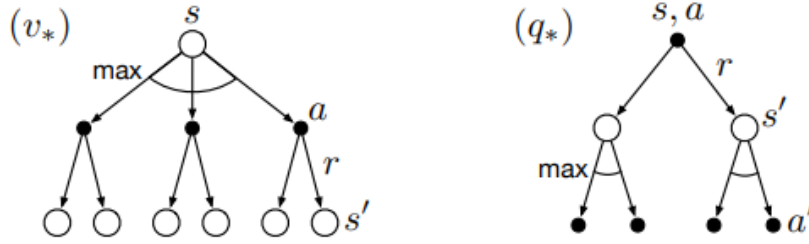


Figure 2.2: Backup diagrams for v_* and q_* . Source: Sutton and Barto (2018, p. 64).

learning to make good decisions for frequently encountered states at the expense of infrequently encountered states. The Bellman Optimality Equation for v_π is

$$\begin{aligned}
 v_*(s) &= \max_{a \in \mathcal{A}(s)} q_{\pi_*}(s, a) \\
 &= \max_a \mathbb{E}[R_{t+1} + \gamma v_*(S_{t+1}) \mid S_t = s, A_t = a] \\
 &= \max_a \sum_{s', r} p(s', r \mid s, a) [r + \gamma v_*(s')]. \tag{2.6}
 \end{aligned}$$

and the Bellman Optimality Equation for q_π is given by

$$\begin{aligned}
 q_*(s, a) &= \mathbb{E} \left[R_{t+1} + \gamma \max_{a'} q_*(S_{t+1}, a') \mid S_t = s, A_t = a \right] \\
 &= \sum_{s', r} p(s', r \mid s, a) \left[r + \gamma \max_{a'} q_*(s', a') \right]. \tag{2.7}
 \end{aligned}$$

The backup diagram on the left of fig. 2.2 graphically represents eq. (2.6), and the backup diagram on the right of fig. 2.2 graphically illustrates eq. (2.7).

2.2.3 Optimal Value Functions and Optimal Policies

Solving a RL task roughly means finding a policy that achieves a lot of reward over the long run. Value functions define a partial ordering over policies: a policy π is defined to be better than or equal to a policy π' if its expected return is greater or equal to that of π' for all states, meaning $\pi \geq \pi'$ if and only if $v_\pi(s) \geq v_{\pi'}(s)$ for all $v \in \mathcal{S}$. At least one policy is always better than or equal to all other policies; we call it the *optimal policy*. Although there may be more than one, we denote all the optimal policies by π_* . They all share the same state-value function, called the *optimal state-value function*.

Definition 2.2.3 (Optimal state-value function). The *optimal state-value function* $v_*(s)$ is the maximum state-value function over all policies.

$$v_*(s) \doteq \max_{\pi} v_{\pi}(s), \text{ for all } s \in \mathcal{S}.$$

Definition 2.2.4 (Optimal action-value function). The *optimal action-value function* $q_*(s, a)$ is the maximum action-value over all policies.

$$q_*(s, a) \doteq \max_{\pi} q_{\pi}(s, a), \text{ for all } s \in \mathcal{S} \text{ and } a \in \mathcal{A}(s).$$

Theorem 2.2.1 (Optimal policies). *For any Markov Decision Process:*

- *There exists an optimal policy π_* that is better than or equal to all other policies, $\pi_* \geq \pi, \forall \pi$*
- *There is always a deterministic optimal policy*
- *All optimal policies achieve the optimal value function $v_{\pi_*}(s) = v_*(s)$*
- *All optimal policies achieve the optimal action-value function $q_{\pi_*}(s, a) = q_*(s, a)$*

Any policy that is greedy with respect to the optimal evaluation function v_* is an optimal policy; this implies that a one-step-ahead search using v_* yields long-term optimal actions. Similarly, by utilising q_* , the agent can bypass the need for this one-step look ahead; it only needs to choose any action that maximises $q_*(s, a)$ without knowledge about the environment's dynamics. Hence, an optimal policy can be found by maximising over $q_*(s, a)$,

$$\pi_*(a|s) = \begin{cases} 1 & \text{if } a = \arg \max_{a \in \mathcal{A}(s)} q_*(s, a) \\ 0 & \text{otherwise} \end{cases} \quad (2.8)$$

2.2.4 Advantage Function

Sometimes, in RL, we do not need to describe how good an action is in an absolute sense, but only how much better it is than others on average. That is to say, we want to know the relative advantage of that action. We make this concept precise with the *advantage function*.

Definition 2.2.5 (Advantage function). The advantage function $A_{\pi}(s, a)$ corresponding to a policy π describes how much better it is to take a specific action a in state s over randomly selecting an action according to $\pi(\cdot|s)$, assuming you act according to π forever after.

$$A_{\pi}(s, a) = q_{\pi}(s, a) - v_{\pi}(s).$$

2.2.5 Exploration and Exploitation Trade-off

A central theme of RL is the balance between exploitation — meaning leveraging past experiences to obtain reward — and exploration, which we use to discover better action selections in the future. The agent must, therefore, balance the two to complete the task by trying a variety of actions and then progressively favouring those that appear to be best. The exploration-exploitation dilemma has been intensively studied but remains unsolved (Sutton & Barto, 2018).

2.3 Model-Free and Model-Based

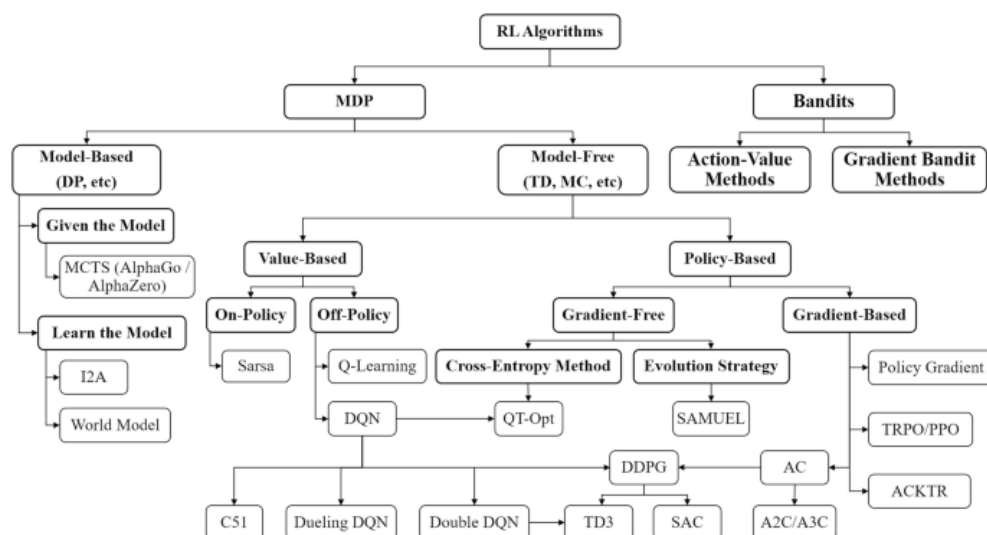


Figure 2.3: A taxonomy of Reinforcement Learning methods and algorithms. Source: Zhang and Yu (2020).

One of the most crucial branching points in an RL algorithm is whether the agent has access to a model of the environment. By a model of the environment, we mean a function which predicts state transitions and rewards. The model may be either given a priori or learned through experience. The main upside to having a model is that it allows the agent to plan by thinking ahead, seeing what would happen for a range of possible choices, and explicitly deciding between its options. Agents can then distil the results from planning ahead into a learned policy. A particularly famous example of this approach is Silver et al. (2017), where AlphaGo Zero is given an exact model of the game of Go. When this works, it can substantially improve sample

efficiency over methods that do not have a model. The main downside is that a ground-truth model of the environment is usually not available. If an agent wants to use a model in this case, it has to learn it purely from experience, which creates several challenges. MuZero gives an example of successful model-learning in Silver et al. (2018). However, the biggest challenge is that bias in the model can be exploited by the agent, resulting in an agent which performs well with respect to the learned model but behaves sub-optimally or terribly in the real environment. Model learning is fundamentally hard, so even considerable investments of time and computational resources can fail to pay off. Algorithms which use a model are called *model-based methods*, and those that do not are called *model-free methods*. A potential classification of RL algorithms is given in fig. 2.3. While model-free methods forego the potential gains in sample efficiency from using a model, they tend to be easier to implement and tune. This thesis predominantly explores model-free methods, focusing on their practicality in RL.

Chapter 3

Reinforcement Learning Algorithms

This chapter gives an overview of the RL algorithms, starting with the basic tabular methods and leading up to the function approximation case. We begin by explaining value-based methods, including the central concepts of prediction, control and policy iteration. We show and explain the classic off-policy Q-learning algorithm. Later, we generalise value-based methods to the function approximation case using semi-gradient methods. We show the extension of tabular Q-learning to the famous DQN. We then introduce policy gradient methods using REINFORCE as an example, which we modify by adding a baseline to move closer to actor-critic methods. We then show and detail the A2C algorithm, which combines policy gradient and value-based methods. We conclude by showing PPO, a state-of-the-art actor-critic algorithm that improves upon A2C.

There are two main approaches to representing and training agents, *Policy Optimisation methods* and *Value-based methods* (sometimes referred to as *Q-Learning methods*). Methods in Policy Optimisation represent a policy explicitly as $\pi(a|s, \theta)$. They optimise the parameters θ directly by gradient ascent on the performance objective $J(\theta)$ or indirectly by maximising local approximations of $J(\theta)$. This optimisation is almost always performed on-policy, which means that each update only uses data collected while acting according to the most recent version of the policy. Policy optimisation also usually involves learning an approximator $\hat{v}(s, \mathbf{w})$ for the on-policy value function $v_\pi(s)$, which gets used to help with policy updates. Methods such as A2C and 1PPO fall under this category. Value-based approaches predominantly focus on learning an approximator $\hat{q}(s, a, \mathbf{w})$ for the optimal action-value function, $q_*(s, a)$. The objective function used is typically derived from the Bellman equation. Optimisation under this method is often conducted

off-policy, meaning that each update can use data collected at any point during training, regardless of how the agent chose to explore the environment when the data was obtained. The resultant policy is obtained through the relationship between q_* and π_* , as shown in eq. (2.8) on page 16. DQN is a notable example of value-based methods. The primary strength of policy optimisation methods is their principled nature, in the sense that they directly optimise for the desired outcome. This tends to make them stable and reliable. By contrast, value-based methods only indirectly optimise agent performance by training \hat{q} to satisfy a self-consistency equation. This kind of learning has many failure modes, so it tends to be less stable. However, value-based methods gain the advantage of being substantially more sample efficient when they do work because they can reuse data more effectively than policy optimisation techniques (Achiam, 2018).

3.1 Value-based Methods

In value-based methods, we try to learn an optimal policy indirectly represented through value functions. DP provides an essential foundation and collection of algorithms based on value-based methods. Value-based methods can be viewed as attempts to achieve the same goal as DP, only with less computation and without assuming a perfect model of the environment. In value-based methods, we use value functions to organise and structure the search for good policies: we find an optimal value function, which is then used to derive an optimal policy for the agent. The goal is to learn a function that assigns a value to each state or to each state-action pair such that the value function accurately represents the expected return starting from that state (or state-action pair) and acting optimally thereafter.

3.1.1 Policy Iteration

We can use v_π to improve π and yield a better policy π' , and we can repeat this process by computing $v_{\pi'}$ and to generate an even better policy π'' . We can thus obtain a sequence of monotonically improving policies and value functions. Each policy is guaranteed to be a strict improvement over the previous one (unless it is already optimal). Because a finite MDP has only a finite number of deterministic policies, this process must converge to an optimal policy and the optimal value function in a finite number of iterations. As discussed before in section 2.2.3 on page 15, we can easily obtain the optimal policies once we have found the optimal value functions, namely v_* and q_* , which satisfy the Bellman optimality equations shown in section 2.2.2

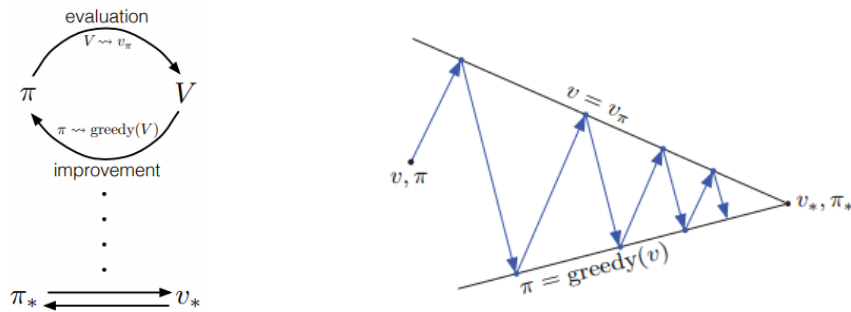


Figure 3.1: The interaction between evaluation and improvement processes in GPI. Source: Sutton and Barto (2018, pp. 86–87).

on page 14. To do so, we use a technique called *policy iteration*, which is the foundation of all value-based methods in RL:

1. *Policy evaluation*, also known as *prediction*, is where we iteratively compute the value function for a given policy.
2. *Policy improvement*, also known as *control*, is where we compute an improved policy given the value function for that policy.

In policy iteration, we first use policy evaluation to fully compute the value function v_π for a given policy until convergence. Then we apply policy improvement where we gradually build a new, improved policy π' by greedily selecting actions from v_π by visiting every state until π' has converged. *Generalised Policy Iteration (GPI)* is a generalisation of policy iteration, where we do approximate policy evaluation and approximate policy improvement. One process takes the policy as given and performs some form of policy evaluation, changing the value function to be more like the true value function for the policy. The other process takes the value function as given. It performs some form of policy improvement, changing the policy to improve it, assuming that the value function is its value function. A policy or value function that remains unchanged by either process is optimal, and thus, it has converged. *Value iteration* is a special case of GPI where the policy evaluation is stopped after just one sweep of the state space: both GPI and value iteration have been proven to converge with the same guarantees as policy iteration.

3.1.2 Generalised Policy Iteration

Policy iteration consists of two simultaneous, interacting processes, one making the value function consistent with the current policy, called policy eval-

uation, and the other making the policy greedy with respect to the current value function, policy improvement. In policy iteration, these two processes alternate, each completing before the other begins, but this is unnecessary. In value iteration, for example, only a single iteration of policy evaluation is performed between each policy improvement. Sometimes, a single state is updated in one process before returning to the other. As long as both processes continue to update all states, the ultimate result is typically the same—convergence to the optimal value function and an optimal policy. We use the term Generalised Policy Iteration (GPI) to refer to the general idea of letting policy-evaluation and policy improvement processes interact, independent of the granularity and other details of the two processes. Almost all RL methods are well described as GPI. All have identifiable policies and value functions, with the policy continuously being improved with respect to the value function and the value function always being driven toward the value function for the policy, as suggested by fig. 3.1. If both the evaluation and improvement processes stabilise and no longer produce changes, then the value function and policy must be optimal. The value function stabilises only when it is consistent with the current policy, and the policy stabilises only when it is greedy with respect to the current value function. Thus, both processes stabilise only when a policy is greedy with respect to its own evaluation function. This implies that the Bellman optimality equation eq. (2.6) on page 15 holds, and thus, the policy and the value function are optimal.

3.1.3 On-policy and Off-policy Methods

In *on-policy* algorithms, the agent learns the value function $v_\pi(s)$ or the action-value function $q_\pi(s)$ with respect to the policy π that it is currently executing. In *off-policy* algorithms, the agent learns the value function $v_\pi(s)$ or the action-value function $q_\pi(s)$ for a deterministic optimal policy π^* that may be unrelated to the policy followed. The policy that generates the data is called the *behaviour policy* b , whereas the *target policy* π is the policy whose value function we want to learn. Since we use data from the behaviour policy to update a different target policy, methods such as *importance sampling* are often needed to offset this mismatch. Thus, off-policy methods are often of greater variance and are slower to converge than on-policy methods. They are also particularly problematic when it comes to function approximation, as it will be later explained in section 3.2.3.

The Exploration Dilemma

As mentioned in section 2.2.5 on page 17 and section 3.1.2, learning control methods face a dilemma: they seek to learn action values conditional on subsequent optimal behaviour, but they need to behave non-optimally to explore all actions and find the optimal actions. On-policy and off-policy methods use two different approaches to learn about the optimal policy while behaving according to an exploratory policy. In on-policy methods, the exploration-exploitation tradeoff is particularly delicate, as the agent needs to find a near-optimal policy that still explores. The most straightforward idea for ensuring continual exploration is to make the policy *soft* so that $\pi(a|s) > 0$ for all $s \in \mathcal{S}$ and all $a \in A(s)$, but gradually shifted closer and closer to a deterministic optimal policy. The ϵ -*greedy* policy is the ϵ -soft policy that is closer to the greedy policy. It has probability ϵ to select an action at random and $1 - \epsilon + \frac{\epsilon}{|A(s)|}$ probability to select the greedy action. Guaranteeing exploration in off-policy methods seems more straightforward since the target policy can be an optimal greedy policy, whilst behaviour policy can be an exploratory ϵ -*greedy* policy.

3.1.4 Monte Carlo Methods

Monte Carlo (MC) methods are ways of solving the RL problem based on averaging sample returns. MC methods do not assume complete knowledge of the environment dynamics as they only require experience, meaning sample sequences of states, actions and rewards from actual or simulated interaction with an environment. A model is required only to generate sample transitions, not the complete probability distributions of all transitions required for DP. We refer to "Monte Carlo" as methods based on averaging *complete* returns, underlining the offline nature of these methods since they require complete episode rollouts. The first advantage of MC methods is that they can be used to learn optimal behaviour directly from the environment, with no model of the environment's dynamics. Second, they can be used with simulation or sample models. Third, it is easy and efficient to focus MC methods on a small subset of states that are of specific interest. A fourth advantage is that violations of the Markov property may less harm them because they do not bootstrap, meaning they do not use the Bellman equations consistency property for their updates. MC control methods still follow the overall schema of GPI.

3.1.5 Temporal-Difference Methods

TD learning is a core and innovative aspect of RL that combines MC aspects with DP principles. Like MC methods, TD methods can learn directly from raw experience without a model of the environment's dynamics. Like DP, TD methods update estimates based partly on other learned estimates without waiting for the outcome. The general idea of updating estimates based on other estimates is called *bootstrapping*. Whereas MC methods must wait until the end of the episode to compute the return G_t and determine the increment to $V(S_t)$, TD methods need to wait only until the next timestep. At time $t + 1$, they immediately form a target and make a useful update using the observed reward R_{t+1} and the estimate $V(S_{t+1})$. The simplest form of TD learning is a one-step method that makes the update

$$V(S_t) \leftarrow V(S_t) + \alpha [R_{t+1} + \gamma V(S_{t+1}) - V(S_t)] \quad (3.1)$$

immediately on transition to S_{t+1} and receiving R_{t+1} . We call $R_{t+1} + \gamma V(S_{t+1})$ the *TD target* and we define δ_t as

$$\delta_t \doteq R_{t+1} + \gamma V(S_{t+1}) - V(S_t) \quad (3.2)$$

the *TD error*, which is used in various forms in many RL algorithms.

We use the GPI to build an on-policy TD control method that uses the action-value function rather than the state-value function in eq. (3.1) for the TD update:

$$Q(S_t, A_t) \leftarrow Q(S_t, A_t) + \alpha [R_{t+1} + \gamma Q(S_{t+1}, A_{t+1}) - Q(S_t, A_t)]. \quad (3.3)$$

This leads to the State–action–reward–state–action (SARSA) control method shown in algorithm 1. Note that the "(0)" notation refers to the fact that this is the one-step version. In general, TD methods try to find estimates that would be correct for the Markov process's maximum-likelihood model. The maximum-likelihood estimate of a parameter is the parameter value whose probability of generating the data is greatest. In contrast, MC methods find the estimates that minimise the mean-squared error on the training set. This is why, despite being biased, TD methods typically converge more quickly than MC. At the same time, this makes TD methods more fragile to violations of the Markov property.

Algorithm 1 SARSA(0), On-policy TD Control

- 1: Initialize $Q(s, a)$ for all $s \in \mathcal{S}$, $a \in \mathcal{A}(s)$, arbitrarily except that $Q(\text{terminal state}, \cdot) = 0$
 - 2: **for** each episode **do**
 - 3: Initialize S
 - 4: Choose A from S using policy derived from Q (e.g., ϵ -greedy)
 - 5: **for** each step of episode **do**
 - 6: Take action A , observe R, S'
 - 7: Choose A' from S' using policy derived from Q (e.g., ϵ -greedy)
 - 8: $Q(S, A) \leftarrow Q(S, A) + \alpha[R + \gamma Q(S', A') - Q(S, A)]$
 - 9: $S, A \leftarrow S', A'$
-

3.1.6 Q-Learning

One of the early breakthroughs in RL was the development of an off-policy TD control algorithm known as *Q-learning* (Watkins & Dayan, 1992), whose update rule is defined by:

$$Q(S_t, A_t) \leftarrow Q(S_t, A_t) + \alpha \left[R_{t+1} + \gamma \max_a Q(S_{t+1}, a) - Q(S_t, A_t) \right]. \quad (3.4)$$

Here, the learned action-value function Q directly approximates q_* independent of the policy being followed; hence the method being off-policy. Q-learning follows the pattern of value iteration described in section 3.1.1 and is implemented in algorithm 2.

Algorithm 2 Q-Learning, Off-policy TD Control

- 1: Initialise $Q(s, a)$ for all $s \in \mathcal{S}$, $a \in \mathcal{A}(s)$, arbitrarily except that $Q(\text{terminal state}, \cdot) = 0$
 - 2: **for** each episode **do**
 - 3: Initialise S
 - 4: **for** each step of episode **do**
 - 5: Choose action A using policy derived from Q (e.g., ϵ -greedy)
 - 6: Take action A , observe R, S'
 - 7: $Q(S, A) \leftarrow Q(S, A) + \alpha[R + \gamma \max_a Q(S', a) - Q(S, A)]$
 - 8: $S \leftarrow S'$
-

3.2 Value-based Methods with Approximation

In value-based methods, the approximate value function is represented as a parametrised functional form with weight vector $\mathbf{w} \in \mathcal{R}^d$. We write $\hat{v}(s, \mathbf{w}) \approx$

$v_\pi(s)$ for the approximate value of state s given vector \mathbf{w} . Usually, \hat{v} is the function computed by a multi-layer AAN, with \mathbf{w} the vector of connection weights in all the layers. Typically, the number of weights (the dimensionality of \mathbf{w}) is much less than the number of states ($d \ll |\mathcal{S}|$), and changing one weight changes the estimated value of many states. Consequently, when a single state is updated, the change generalises from that state to affect the values of many other states. This generalisation makes the learning potentially more powerful but potentially more challenging to manage and understand.

However, not all function approximation methods are equally well suited for use in RL. The most sophisticated artificial neural network and statistical methods assume a static training set over which multiple passes are made. In RL, it is vital that learning be able to occur online while the agent interacts with its environment or with a model of its environment. To do this requires methods that can learn efficiently from incrementally acquired data. In addition, RL generally requires function approximation methods to handle nonstationary target functions (target functions that change over time). For example, in control methods based on GPI, we often seek to learn q_π while π changes. Even if the policy remains the same, the target values of training examples are nonstationary if they are generated by bootstrapping methods (such as DP and TD learning). Methods that cannot easily handle such nonstationarity are less suitable for RL.

To define an explicit learning objective for prediction, we must then say which states we care most about, as making one state's estimate more accurate invariably means making others' less accurate (by assumption, we have far more states than weights). We must specify a state distribution $\mu(s) \geq 0, \sum_s \mu(s) = 1$, representing how much we care about the error in each state s error. We define the error in a state s as the mean square of the difference between the approximate value $\hat{v}(s, \mathbf{w})$ and the true value $v_\pi(s)$, and we weight this over the state space by μ . We obtain a natural objective function, the *mean square value error*.

Definition 3.2.1 (Mean Square Value Error).

$$\overline{\text{VE}}(\mathbf{w}) \doteq \sum_{s \in \mathcal{S}} \mu(s) [v_\pi(s) - \hat{v}(s, \mathbf{w})]^2,$$

where $\mu(s)$ is called the *on-policy distribution* and is chosen as the fraction of time spent in s under policy π .

It is not completely clear that the $\overline{\text{VE}}$ is the right performance objective for RL. The ultimate purpose and the reason we are learning a value function is to find a better policy. The best value function for this purpose is

not necessarily the best for minimizing $\overline{\text{VE}}$. Nevertheless, it is not yet clear what a more useful alternative goal for value prediction might be. Complex function approximators may seek to converge instead to a local optimum, a weight vector \mathbf{w}^* for which $\overline{\text{VE}}(\mathbf{w}^*) \leq \overline{\text{VE}}(\mathbf{w})$ for all \mathbf{w} in some neighbourhood of w^* . This is typically the best that can be said for nonlinear function approximators. For many cases of interest in RL, there is no guarantee of convergence to an optimum or even to within a bounded distance of an optimum. Some methods may diverge, with their $\overline{\text{VE}}$ approaching infinity in the limit.

3.2.1 Stochastic-gradient Methods

To minimise $\overline{\text{VE}}$, we typically use methods based on *Stochastic Gradient Descent (SGD)*, which are well suited to online RL. A common strategy is to minimise the $\overline{\text{VE}}$ on observed examples, which we can do by using SGD to adjust the weight vector \mathbf{w} after each example by a small amount in the direction that would most reduce the error on that example:

$$\mathbf{w}_{t+1} \doteq \mathbf{w}_t - \frac{1}{2}\alpha \nabla [v_\pi(S_t) - \hat{v}(S_t, \mathbf{w}_t)]^2 \quad (3.5)$$

$$= \mathbf{w}_t + \alpha [v_\pi(S_t) - \hat{v}(S_t, \mathbf{w}_t)] \nabla \hat{v}(S_t, \mathbf{w}_t) \quad (3.6)$$

where α is a positive step-size parameter, also called the *learning rate*.

3.2.2 Semi-gradient Methods

One problem with eq. (3.6) is that in practice, we do not have the true value $v_\pi(S_t)$ but some, possibly random or bootstrapped, approximation to it. Therefore, we cannot perform an exact update because $v_\pi(S_t)$ is unknown, but we can approximate it using a target estimate U_t . If U_t is an unbiased estimate, meaning that $\mathbb{E}[U_t|S_t = s] = v_\pi(s)$ for each t , then \mathbf{w}_t is guaranteed to converge to a local optimum under SGD. An example of an unbiased estimate would be the MC target $U_t \doteq G_t$. If a bootstrapping estimate of $v_\pi(S_t)$ is used as the U_t , such as in TD methods, then U_t will also depend on the current value of the weight vector \mathbf{w}_t , which implies that they will be biased and will not produce a true gradient-descent method. The step from eq. (3.5) to eq. (3.6) relies on the target being independent of \mathbf{w}_t and would not be valid if a bootstrapping estimate were used in place of $v_\pi(S_t)$. Bootstrapping methods consider the effect of changing the weight vector \mathbf{w}_t on the estimate but ignore its effect on the target. Because they include only a part of the gradient, they are accordingly called *semi-gradient methods*. Semi-

gradient methods are still preferred for the usual reason that bootstrapped estimates enable significantly faster online learning.

We now extend the SARSA algorithm in algorithm 1 to function approximation. Similarly to what we did for eq. (3.3), we use the update rule for the state-value function in eq. (3.6) to derive an update rule using the approximate action-value function instead:

$$\mathbf{w}_{t+1} \doteq \mathbf{w}_t + \alpha [R_{t+1} + \gamma \hat{q}(S_{t+1}, A_{t+1}, \mathbf{w}_t) - \hat{q}(S_t, A_t, \mathbf{w}_t)] \nabla \hat{q}(S_t, A_t, \mathbf{w}_t). \quad (3.7)$$

We have now obtained the update rule for the semi-gradient one-step on-policy control SARSA in algorithm 3.

Algorithm 3 Semi-gradient SARSA(0), On-policy TD Control

- 1: Input: a differentiable function $\hat{q} : \mathcal{S} \times \mathcal{A} \times \mathbb{R}^d \rightarrow \mathbb{R}$
 - 2: Initialise value-function weights \mathbf{w} arbitrarily \mathbb{R}^d (e.g., $\mathbf{w} = \mathbf{0}$)
 - 3: **for** each episode **do**
 - 4: Initialise S, A (first state and action)
 - 5: **for** each step of episode **do**
 - 6: Take action A , observe R, S'
 - 7: **if** S' is terminal **then**
 - 8: $\mathbf{w} \leftarrow \mathbf{w} + \alpha [R - \hat{q}(S, A, \mathbf{w})] \nabla \hat{q}(S, A, \mathbf{w})$
 - 9: Go to the next episode
 - 10: Choose A' as a function of $\hat{q}(S', \cdot, \mathbf{w})$ (e.g., ϵ -greedy)
 - 11: $\mathbf{w} \leftarrow \mathbf{w} + \alpha [R + \gamma \hat{q}(S', A', \mathbf{w}) - \hat{q}(S, A, \mathbf{w})] \nabla \hat{q}(S, A, \mathbf{w})$
 - 12: $S, A \leftarrow S', A'$
-

3.2.3 Function Approximation with Off-policy Methods

The extension to function approximation turns out to be significantly different and harder for off-policy learning than it is for on-policy learning. The tabular off-policy methods readily extend to semi-gradient algorithms, but these algorithms do not converge as robustly as they do under on-policy training. The fact that the distribution of updates in the off-policy case is not according to the on-policy distribution creates additional problems. Two general approaches have been explored to deal with this. One is to use importance sampling methods to warp the update distribution back to the on-policy distribution. The other is to develop true gradient methods that do not rely on any special distribution for stability, which we will not cover here.

By changing their update rule, we can easily convert algorithm 2 and algorithm 3 to off-policy semi-gradient form. For the one-step off-policy semi-gradient SARSA we need to introduce the *per-step importance sampling ratio* ρ_t :

$$\rho_t \doteq \frac{\pi(A_t|S_t)}{b(A_t|S_t)}. \quad (3.8)$$

Then we change the update rule of eq. (3.7) to be:

$$\mathbf{w}_{t+1} \doteq \mathbf{w}_t + \alpha \rho_t [R_{t+1} + \gamma \hat{q}(S_{t+1}, A_{t+1}, \mathbf{w}_t) - \hat{q}(S_t, A_t, \mathbf{w}_t)] \nabla \hat{q}(S_t, A_t, \mathbf{w}_t).$$

In the case of Q-learning, we do not need importance sampling, as the update rule eq. (3.4) matches exactly what the target policy is doing, namely learning about the optimal greedy policy. As a result, the update remains the same:

$$\mathbf{w}_{t+1} \doteq \mathbf{w}_t + \alpha \left[R_{t+1} + \gamma \max_a \hat{q}(S_{t+1}, a, \mathbf{w}_t) - \hat{q}(S_t, A_t, \mathbf{w}_t) \right] \nabla \hat{q}(S_t, A_t, \mathbf{w}_t) \quad (3.9)$$

Tsitsiklis and Van Roy (1997) has shown that off-policy Q-learning with non-linear function approximations can cause the Q-network to diverge, despite non-gradient Q-learning having the best convergence guarantees of all control methods (Sutton & Barto, 2018). This shows the dangers and instability of using approximations combined with off-policy methods. In particular, Sutton and Barto (2018) shows how divergence arises whenever we combine all of the following three elements, called *the deadly triad*: 1. Function approximation 2. Bootstrapping and 3. Off-policy training.

3.2.4 Deep Q-Learning

We now introduce Deep Q-Network (DQN), a DRL algorithm first shown in Mnih et al. (2013), Mnih et al. (2015), that generalises Q-learning to the function approximation case. In 3.2.3 we have talked about the instability and divergence of Q-learning with function approximation. DQN attempts to mitigate these issues using a number of enhancements. First of all, it uses a *minibatch method* that updates weights only after accumulating gradient information over a set threshold of observation. The original implementation used a gradient-ascent algorithm called RMSProp, but modern implementations (including the one we use in this thesis) often use Adam instead (Kingma & Ba, 2015). Moreover, it modifies the classic Q-learning algorithm in three ways. (1) Through the use of a method called *experience replay*, it stores the agent's experience in a replay memory \mathcal{D} that is accessed to perform the weight updates. At each timestep, a transition including the agent's actions, the observation and the reward are added to \mathcal{D} . Then, a minibatch

update is performed based on experiences *sampled uniformly at random* from \mathcal{D} . Instead of S_{t+1} becoming the new S_t for the next update as in usual Q-learning, a new unconnected experience is drawn from \mathcal{D} to supply data for the next update. This is enabled by the fact that Q-Learning is an off-policy algorithm. Thanks to experience replay DQN gains several advantages over Q-Learning. First, it benefits from increased sample efficiency, as experiences are stored and used for many updates instead of being immediately discarded after the update. Second, it reduces the variance of the updates because successive updates are not correlated with one another as they would normally be. By removing the dependence of successive experiences on the current weights it eliminates one source of instability. (2) A modified version of eq. (3.9) with *fixed Q-targets* is used to further improve stability. As seen in section 3.2.2, Q-learning is a semi-gradient method whose update rule depends on a bootstrapped action-value function estimate. The problem with semi-gradient methods is that the target is a function of the same parameters that are being updated and this can lead to oscillations and divergence. Another Q-network called the *target network* is used to address this. After a certain number of updates C to the weights \mathbf{w} , the online network's current weights are inserted into the target network. The weights of the target network are then held fixed for the next C updates of \mathbf{w} . This additional fixed network is then used to compute the Q-learning targets, thus avoiding the "moving Q-targets" problem. The update rule changes as follows:

$$\mathbf{w}_{t+1} \doteq \mathbf{w}_t + \alpha \left[R_{t+1} + \gamma \max_a \hat{q}_{tg}(S_{t+1}, a, \mathbf{w}_t) - \hat{q}(S_t, A_t, \mathbf{w}_t) \right] \nabla \hat{q}(S_t, A_t, \mathbf{w}_t), \quad (3.10)$$

where $q_{tg}(s, a, \mathbf{w}_t)$ indicates the action-value estimate of the target Q-network. (3) A final modification that improves the stability of standard Q-learning is the clipping of the TD error $R_{t+1} + \gamma \max_a \hat{q}_{dup}(S_{t+1}, a, \mathbf{w}_t) - \hat{q}(S_t, A_t, \mathbf{w}_t)$ so that it remains in the interval $[-1, 1]$. We show the pseudocode for DQN in algorithm 4. The original DQN has been substantially improved over the next years by using additional tricks to further stabilise learning. One of the problems of both classic Q-learning and DQN is the *maximisation bias*. This stems from the fact that a maximum overestimated value is implicitly used to estimate the maximum value, which leads to significant positive bias. For instance, consider a state where all the actions have zero true values but whose action-value estimates are distributed, some above and some below zero. The maximum of the true values is zero, but the maximum of the estimates is positive, leading to positive bias. van Hasselt et al. (2016) overcomes this problem by decoupling action selection to action evaluation. The greedy policy is evaluated according to the online network but uses the target

Algorithm 4 Deep Q-Learning with Experience Replay

```

1: Initialise replay memory  $\mathcal{D}$  to capacity  $N$ 
2: Initialise action-value function  $\hat{q}$  with random weights  $\theta$ 
3: Initialise target action-value function  $\hat{q}_{tg}$  with weights  $\theta^- = \theta$ 
4: for episode = 1,  $M$  do
5:   Initialize state  $S$ 
6:   for timestep  $t = 1, T$  do
7:     With probability  $\epsilon$  select a random action  $A$ 
8:     Otherwise select  $A = \arg \max_a \hat{q}(s, a, \theta)$ 
9:     Take action  $A$ , observe  $R, S'$ 
10:    Store transition  $(S, A, R, S')$  in  $\mathcal{D}$ 
11:    Sample random mini-batch of transitions from  $\mathcal{D}$ 
12:    for each  $(S, A, R, S')$  do
13:      if  $S'$  is terminal then
14:         $y_j = R$ 
15:      else
16:         $y_j = R + \gamma \max_{a'} \hat{q}_{tg}(S', A', \theta^-)$ 
17:      Perform a gradient descent step on  $(y_j - \hat{q}(s, a, \theta))^2$  with respect
        to the parameters  $\theta$ 
18:    Every  $C$  steps reset  $\hat{q}_{tg} = \hat{q}$ 

```

network to estimate its value. The DQN update changes to:

$$\mathbf{w}_{t+1} \doteq \mathbf{w}_t + \alpha \left[R_{t+1} + \gamma \hat{q}_{tg}(S_{t+1}, \arg \max \hat{q}(S_t, A_t, \mathbf{w}_t), \mathbf{w}_t) - \hat{q}(S_t, A_t, \mathbf{w}_t) \right] \nabla \hat{q}(S_t, A_t, \mathbf{w}_t),$$

and leads to significantly better performance. Another notable improvement to DQN is the use of *Prioritised Experience Replay* (Schaul et al., 2016). Instead of sampling the replay buffer uniformly at random, the experiences in \mathcal{D} are sampled with respect to assigned priorities based on the magnitude of their TD error δ , where higher $|\delta|$ values indicate that the experience is surprising and could result in significant Q-value updates. Even more improvements to DQN have been added over the years, culminating in the RAINBOW algorithm (Hessel et al., 2018), which is a version of DQN that includes all improvements up to that date, namely what listed before with the addition of Dueling DQN, multi-step learning, distributional DQN and noisy nets.

3.3 Policy Gradient Methods

Policy gradient methods directly learn a *parametrised policy* that can select actions without consulting a value function. A value function may still be used to learn the policy parameter but is not required for action selection. We use the notation $\boldsymbol{\theta} \in \mathcal{R}^d$ for the policy’s parameter vector and $\pi(a|s, \boldsymbol{\theta}) = \Pr\{A_t = a \mid S_t = s, \boldsymbol{\theta}_t = \boldsymbol{\theta}\}$ for the probability that action a is taken at time t given the environment is in state s at time t with parameter $\boldsymbol{\theta}$. If a method also uses a value function, then the value function’s weight vector is denoted $\mathbf{w} \in \mathcal{R}^d$.

We also define $J(\boldsymbol{\theta})$ as the *objective function*, a scalar performance measure with respect to the policy parameter. Policy gradient methods seek to maximise performance, so their updates approximate gradient *ascent* in J :

$$\boldsymbol{\theta}_{t+1} = \boldsymbol{\theta}_t + \alpha \widehat{\nabla J(\boldsymbol{\theta})}, \quad (3.11)$$

where $\widehat{\nabla J(\boldsymbol{\theta})} \in \mathcal{R}^d$ is a stochastic estimate whose expectation approximates the gradient of the objective function with respect to its argument $\boldsymbol{\theta}_t$. All methods that follow this general schema are called *policy gradient methods*: this includes *actor-critic methods*, which will be explained in section 3.4. Policy gradient methods follow the exact policy gradient and thus usually have better convergence guarantees than semi-gradient methods in section 3.2.2.

3.3.1 The Policy Gradient Theorem

We define the objective function as:

$$J(\boldsymbol{\theta}) \doteq v_{\pi_{\boldsymbol{\theta}}}(s_0) = \mathbb{E}_{\pi_{\boldsymbol{\theta}}} [G_t \mid S_t = s_0],$$

that is, the objective is to learn a policy that maximises the cumulative future reward to be received, starting from an initial state s_0 . We assume an episodic case with no discounting ($\gamma = 1$), but it can be extended for continuing discounted tasks. Thanks to the *policy gradient theorem* (theorem 3.3.1), we have an analytic expression for the gradient of the objective function with respect to the policy parameter that does not involve the derivative of the state distribution $\mu(s)$.

Theorem 3.3.1 (The Policy Gradient Theorem). *The policy gradient theorem for the episodic case is:*

$$\nabla J(\boldsymbol{\theta}) \propto \sum_s \mu(s) \sum_a q_{\pi}(s, a) \nabla \pi(a|s, \boldsymbol{\theta}),$$

where π denotes the policy corresponding to parameter vector $\boldsymbol{\theta}$, the constant of proportionality is the average episode length and μ is the on-policy distribution of states under π .

3.3.2 REINFORCE

We use theorem 3.3.1 to derive the update rule for REINFORCE (Williams, 1992), a classic policy-gradient learning algorithm:

$$\boldsymbol{\theta}_{t+1} = \boldsymbol{\theta}_t + \alpha G_t \nabla \ln \pi(A_t | S_t, \boldsymbol{\theta}_t), \quad (3.12)$$

where $\nabla \ln \pi(A_t | S_t, \boldsymbol{\theta}_t) = \frac{\nabla \pi(A_t | S_t, \boldsymbol{\theta}_t)}{\pi(A_t | S_t, \boldsymbol{\theta}_t)}$.

The right-hand side of eq. (3.12) is a quantity that can be sampled on each time step and whose expectation is proportional to the gradient. Each increment is proportional to the product of a return G_t and a vector, the gradient of the probability of taking the action taken divided by the probability of taking that action A_t on future visits on state S_t . The update increases the parameter vector in this direction proportional to the return and inversely proportional to the action probability. The former makes sense because it causes the parameter to move most in directions, favouring actions that yield the highest return. The latter makes sense because, otherwise, frequently selected actions have an advantage and might win out even if they do not yield the highest return. REINFORCE is a MC algorithm, so all updates are made offline as it needs the complete return from time t , which includes all future rewards up to the end of the episode. REINFORCE has good theoretical convergence properties as the expected update over an episode is in the same direction as the performance gradient. However, as a MC method, it is of high variance and thus produces slow learning. We give the pseudocode in algorithm 5.

Algorithm 5 REINFORCE: Monte-Carlo Policy-Gradient Control

- 1: Input: a differentiable policy parametrisation $\pi(a|s, \boldsymbol{\theta})$
 - 2: Initialise policy parameter $\boldsymbol{\theta} \in \mathbb{R}^{d'}$ arbitrarily
 - 3: **for** each episode **do**
 - 4: Generate an episode $S_0, A_0, R_1, \dots, S_{T-1}, A_{T-1}, R_T$ following $\pi(\cdot | \cdot, \boldsymbol{\theta})$
 - 5: **for** each step of the episode $t = 0, 1, \dots, T - 1$: **do**
 - 6: $G \leftarrow \sum_{k=t+1}^T \gamma^{k-t-1} R_k$
 - 7: $\boldsymbol{\theta} \leftarrow \boldsymbol{\theta} + \alpha \gamma^t G \nabla \ln \pi(A_t | S_t, \boldsymbol{\theta})$
-

3.3.3 REINFORCE with Baseline

The policy gradient theorem 3.3.1 can be generalised to include a comparison of the action value to an arbitrary *baseline* $b(s)$. The baseline $b(s)$ can be any function as long as it does vary with a , such that we can subtract it from the policy gradient without changing expectation:

$$\nabla J(\boldsymbol{\theta}) \propto \sum_s \mu(s) \sum_a (q_\pi(s, a) - b(s)) \nabla \pi(a|s, \boldsymbol{\theta}), \quad (3.13)$$

The policy gradient theorem with baseline eq. (3.13) can be used to derive an update rule for a new version of REINFORCE that includes a general baseline:

$$\boldsymbol{\theta}_{t+1} = \boldsymbol{\theta}_t + \alpha (G_t - b(S_t)) \nabla \ln \pi(A_t|S_t, \boldsymbol{\theta}_t), \quad (3.14)$$

The baseline leaves the expected value of the update unchanged but can significantly affect its variance. In some states, all actions have high values, necessitating a high baseline to help distinguish between the more valuable and less valuable actions. A low baseline is more suitable in other states where all actions hold low values. One natural choice for the baseline is an estimate of the state value, $\hat{v}(S_t, \mathbf{w})$. Because REINFORCE is a MC method for learning the policy parameter $\boldsymbol{\theta}$, we also use MC to learn the state-value function weights \mathbf{w} . Note how in algorithm 6, the learned state-value

Algorithm 6 REINFORCE with Baseline

- 1: Input: a differentiable policy parametrisation $\pi(a|s, \boldsymbol{\theta})$
 - 2: Input: a differentiable state-value function parametrisation $\hat{v}(s, \mathbf{w})$
 - 3: Initialise policy parameter $\boldsymbol{\theta} \in \mathbb{R}^{d'}$ and state-value weights $\mathbf{w} \in \mathbb{R}^d$ arbitrarily
 - 4: **for** each episode **do**
 - 5: Generate an episode $S_0, A_0, R_1, \dots, S_{T-1}, A_{T-1}, R_T$ following $\pi(\cdot|s, \boldsymbol{\theta})$
 - 6: $G \leftarrow 0$
 - 7: **for** $t \leftarrow T-1, T-2, \dots, 0$ **do**
 - 8: $G \leftarrow \sum_{k=t+1}^T \gamma^{k-t-1} R_k$
 - 9: $\delta \leftarrow G - \hat{v}(S_t, \mathbf{w})$
 - 10: $\mathbf{w} \leftarrow \mathbf{w} + \alpha^{\mathbf{w}} \delta \nabla \hat{v}(S_t, \mathbf{w})$
 - 11: $\boldsymbol{\theta} \leftarrow \boldsymbol{\theta} + \alpha^{\boldsymbol{\theta}} \gamma^t \delta \nabla \ln \pi(A_t|S_t, \boldsymbol{\theta})$
-

function estimates the value of only the first state of each state transition. This estimate sets a baseline for the subsequent return but is made before the transition's action and thus cannot be used to assess that action.

3.4 Actor-Critic Methods

Actor-critic policy-gradient methods learn approximations of policy and value functions, where *actor* refers to the learned policy, and *critic* refers to the learned state-value function. The difference with algorithm 6 is that the state-value function is also applied to the *second* state of the transition. The estimated value of the second state is then discounted and added to the reward. It constitutes the one-step return $G_{t:t+1}$, which is a useful estimate of the actual return and can be used to assess the action. The one-step return is often superior to the actual return in terms of its variance and computational complexity, even though it introduces bias.

Here, we examine one-step actor-critic methods that replace the full return of REINFORCE in eq. (3.14) with the one-step return. To estimate the one-step return, we can use any TD method, including Q-learning, TD(0) and SARSA(0). The one-step version is fully online and incremental, meaning that states, actions and rewards are processed as they occur and never revisited. We give a summary of the update rules of classic variants of actor-critic methods, with REINFORCE as a reference:

$$\begin{aligned} \nabla J(\theta) &= \mathbb{E}_\pi [G_t \nabla \log \pi(a_t | s_t)] && \text{(REINFORCE)} \\ \nabla J(\theta) &= \mathbb{E}_\pi [\delta_t \nabla \log \pi(a_t | s_t)] && \text{(SARSA Actor-Critic)} \\ \nabla J(\theta) &= \mathbb{E}_\pi [\hat{q}(S_t, A_t, \mathbf{w}) \nabla \log \pi(a_t | s_t)] && \text{(Q Actor-Critic)} \\ \nabla J(\theta) &= \mathbb{E}_\pi [\hat{A}(S_t, A_t, \mathbf{w}, \mathbf{v}) \nabla \log \pi(a_t | s_t)] && \text{(Advantage Actor-Critic)} \end{aligned}$$

where δ_t is the TD error eq. (3.2) and \hat{A} is the approximate advantage function described in definition 2.2.5 on page 16:

$$\delta_t = R_{t+1} + \gamma \hat{q}(S_{t+1}, A_{t+1}, \mathbf{w}) - \hat{q}(S_t, A_t, \mathbf{w}) \quad (3.15)$$

$$\hat{A}(S_t, A_t, \mathbf{w}, \mathbf{v}) = \hat{q}(S_t, A_t, \mathbf{w}) - \hat{v}(S_t, \mathbf{v}) \quad (3.16)$$

We implement the one-step SARSA Actor-Critic in algorithm 7

Algorithm 7 SARSA(0) Actor-Critic

```

1: Input: differentiable action-value function  $\hat{q}(s, a, \mathbf{w})$  and policy  $\pi(a|s, \boldsymbol{\theta})$ 
   parametrizations
2: Initialize  $\mathbf{w} \in \mathbb{R}^d, \boldsymbol{\theta} \in \mathbb{R}^{d'}$  arbitrarily
3: for each episode do
4:   Initialize  $S$  (first state of episode)
5:    $I \leftarrow 1$ 
6:   Sample  $A \sim \pi(\cdot|S, \boldsymbol{\theta})$ 
7:   for each timestep of episode do
8:     Take action  $A$ , observe  $S', R$ 
9:     Sample  $A' \sim \pi(\cdot|S', \boldsymbol{\theta})$ 
10:     $\delta \leftarrow R + \gamma\hat{q}(S', A', \mathbf{w}) - \hat{q}(S, A, \mathbf{w})$ 
11:     $\mathbf{w} \leftarrow \mathbf{w} + \alpha^{\mathbf{w}}\delta\nabla\hat{q}(S, A, \mathbf{w})$ 
12:     $\boldsymbol{\theta} \leftarrow \boldsymbol{\theta} + \alpha^{\boldsymbol{\theta}}I\delta\nabla\ln\pi(A|S, \boldsymbol{\theta})$ 
13:     $I \leftarrow \gamma I$ 
14:     $S, A \leftarrow S', A'$ 

```

3.4.1 Advantage Actor-Critic

A2C is considered a state-of-the-art algorithm that uses the advantage function as the baseline. The advantage function makes an optimal baseline, as it intuitively indicates how much better it is to take a specific action in a state compared to the average value of that state. We previously defined the advantage function eq. (3.16) to use two distinct approximators to predict state and state-action values separately. However, this is rarely the case in practice, as it would be extremely inefficient. We use the fact that

$$q_{\pi}(s, a) = \mathbb{E}_{\pi} [R_t + \gamma v_{\pi}(S_{t+1}) \mid S_t = s, A_t = a] \quad (3.17)$$

to approximate the advantage function using the TD error computed with a single approximator for the state-value function:

$$\hat{A}(s, a, \mathbf{w}) = r + \gamma\hat{v}(s', \mathbf{w}) - \hat{v}(s, \mathbf{w}). \quad (3.18)$$

Mnih et al. (2016) details an implementation of an asynchronous version of the Advantage Actor-Critic called Asynchronous Advantage Actor-Critic (A3C). However, it was later found that the asynchronous aspect was a hindrance as it only increased the algorithm's complexity with no tangible performance benefits. In Wu et al. (2017), the synchronous version A2C was found to perform better and is now widely adopted. In algorithm 8, we give the pseudocode for a basic version of A2C. A2C is a powerful algorithm that

Algorithm 8 (Synchronous) One-step Advantage Actor-Critic (A2C)

```

1: Input: differentiable state-value function  $\hat{v}(s, \mathbf{w})$  and policy  $\pi(a|s, \boldsymbol{\theta})$ 
   parametrizations
2: Initialize  $\mathbf{w} \in \mathbb{R}^d, \boldsymbol{\theta} \in \mathbb{R}^{d'}$  arbitrarily
3: for each episode do
4:   Initialize  $S$  (first state of episode)
5:    $I \leftarrow 1$ 
6:   for each timestep of episode do
7:     Sample  $A \sim \pi(\cdot|S', \boldsymbol{\theta})$ 
8:     Take action  $A$ , observe  $S', R$ 
9:      $\delta = R + \gamma \hat{v}(S', \mathbf{w}) - \hat{v}(S, \mathbf{w})$ 
10:     $\mathbf{w} \leftarrow \mathbf{w} + \alpha^{\mathbf{w}} \delta \nabla \hat{v}(S, \mathbf{w})$ 
11:     $\boldsymbol{\theta} \leftarrow \boldsymbol{\theta} + \alpha^{\boldsymbol{\theta}} I \delta \nabla \ln \pi(A|S, \boldsymbol{\theta})$ 
12:     $I \leftarrow \gamma I$ 
13:     $S \leftarrow S'$ 

```

can be scaled easily using multiple workers. Its implementations often use workers that collect a small number of transitions in parallel and immediately use them for a single minibatch update, after which the transitions are discarded. These implementations use an n -step version of the Advantage Actor-Critic presented in algorithm 8, where the change would be merely replacing the one-step return G_t with $G_{t:t+n}$, computed by using the transitions stored in transient memory.

3.4.2 Proximal Policy Optimisation (Clip)

PPO (Schulman et al., 2017) is a state of the art actor-critic algorithm based on Trust Region Policy Optimisation (Schulman et al., 2015). Here, we consider the PPO-Clip variant of the algorithm, which is more straightforward to implement and the most widely adopted (Achiam, 2018). PPO updates policies by taking the largest step possible while satisfying a special constraint on how close the new and old policies are allowed to be. This differs from the normal policy gradient, which keeps new and old policies close in parameter space. However, even slight differences in parameter space can substantially differ in performance, so a single bad step can collapse the policy performance. This makes it dangerous to use large step sizes with vanilla policy gradients, thus hurting its sample efficiency. PPO avoids this kind of collapse and quickly and monotonically improves performance. PPO updates maximises a clipped *surrogate objective function* instead of directly indirectly maximising the performance of the policy. By maximizing the surrogate ob-

Algorithm 9 Proximal Policy Optimisation (Clip)

- 1: Initialize $\mathbf{w} \in \mathbb{R}^d, \boldsymbol{\theta} \in \mathbb{R}^{d'}$ arbitrarily
 - 2: **for** each iteration **do**
 - 3: Collect a set of trajectories τ by running policy $\pi(a|s, \boldsymbol{\theta})$
 - 4: Compute rewards-to-go G_t and advantages \hat{A}_t for each τ
 - 5: Store old policy parameters $\boldsymbol{\theta}_{\text{old}}$
 - 6: **for** each optimization epoch **do**
 - 7: **for** each mini-batch (s, a, G, \hat{A}) in τ **do**
 - 8: Compute $r_t(\boldsymbol{\theta}) = \frac{\pi(a|s, \boldsymbol{\theta})}{\pi(a|s, \boldsymbol{\theta}_{\text{old}})}$
 - 9: Compute clipped surrogate objective:

$$L(\boldsymbol{\theta}) = \min \left(r_t(\boldsymbol{\theta}) \hat{A}_t, \text{clip}(r_t(\boldsymbol{\theta}), 1 - \epsilon, 1 + \epsilon) \hat{A}_t \right)$$
 - 10: Update $\boldsymbol{\theta}$ by maximizing $L(\boldsymbol{\theta})$
 - 11: Update \mathbf{w} using G_t
-

jective, it encourages updates that increase the probability of actions that had positive advantages, i.e., were better than the average action in that state according to the old policy, thus encouraging the policy to take more beneficial actions in the future, while simultaneously preventing the policy from changing too drastically and potentially destabilizing the learning process. Before proceeding, we define the probability ratio $r_t(\boldsymbol{\theta})$, similar to the importance sampling ratio we defined in eq. (3.8).

$$r_t(\boldsymbol{\theta}) \doteq \frac{\pi(a|s, \boldsymbol{\theta})}{\pi(a|s, \boldsymbol{\theta}_{\text{old}})}. \quad (3.19)$$

$r_t(\boldsymbol{\theta})$ is used in eq. (3.20) to essentially weigh the advantage of each action by how much more likely it is under the new policy compared to the old policy. PPO maximises the surrogate objective function L^{CLIP} :

$$L^{\text{CLIP}}(\boldsymbol{\theta}) \doteq \mathbb{E} \left[\min \left(r_t(\boldsymbol{\theta}) \hat{A}_t, \text{clip}(r_t(\boldsymbol{\theta}), 1 - \epsilon, 1 + \epsilon) \hat{A}_t \right) \right] \quad (3.20)$$

The clipping in the surrogate objective is governed by the small hyperparameter ϵ , which prevents the policy from changing too much in a single update. If an action's probability under the new policy becomes too different from its probability under the old policy (outside of the range $[1 - \epsilon, 1 + \epsilon]$), the objective is clipped, which prevents the policy from receiving any additional benefit from increasing that action's probability any further. This prevents the policy from changing too drastically and helps maintain policy updates

within a 'trust region', which can prevent the policy from destabilizing due to large updates.

The pseudocode for PPO is given in algorithm 9. Compared to A2C, we see that PPO has better sample efficiency due to having a trajectory buffer \mathcal{D} used for multiple epochs of minibatch SGD updates (or Adam updates, depending on the implementation). Whereas A2C stored transitions in transient memory up to the minibatch size before performing a single update and discarding them, in PPO, the buffer \mathcal{D} is large and contains transitions from multiple trajectories. Following shuffling, these transitions are divided into minibatches to update the policy and value function, and the procedure is repeated across multiple epochs, thereby increasing sample efficiency.

Chapter 4

Related Work

Deep Reinforcement Learning (DRL) has seen rapid and significant advancements in recent years, with environment frameworks pivotal in this progression. These frameworks offer structured, reproducible, and often realistic spaces where algorithms can be trained, verified, and benchmarked. Thanks to these environments, researchers can analyse and compare the performance of DRL agents in various conditions, ranging from simple bidimensional games to highly complex tridimensional simulators. Here, we give an overview of relevant literature concerning both algorithms and environment frameworks. We then conclude the discussion with studies that use DRL techniques to augment agents manipulating objects in physics-based environments.

4.1 Algorithms

Mnih et al. (2013) introduced a DQN model that successfully learned control policies from high-dimensional sensory input using RL. This model maintained a constant architecture and learning algorithm across seven Atari 2600 games from the ALE, outperforming previous approaches and even a human expert in some games, setting a precedent for further exploration and development in RL. Building upon this, Mnih et al. (2015) presented a DQN agent that surpassed the performance of all previous algorithms and achieved human-level play across 49 classic Atari 2600 games using end-to-end DRL. The agent, which used deep CNN architecture and a novel variant of Q-learning, demonstrated robust learning across diverse tasks and showed that it could develop representations supporting adaptive behaviour from high-dimensional sensory inputs. Hester et al. (2018) introduced a deep reinforcement learning algorithm called Deep Q-learning from Demonstrations

(DQfD), which leverages small sets of demonstration data to accelerate the learning process significantly. Unlike prior approaches limited to imitation learning, DQfD combined TD updates with supervised classification of the demonstrator’s actions, enabling it to learn from both demonstration data and self-generated data efficiently. Mnih et al. (2016) proposed A3C, a reinforcement learning method that used parallel actor-learners to stabilise training. A3C stabilised learning and reduced training time and resource requirements by using parallelism. Schulman et al. (2017) introduced PPO algorithms, a family of policy gradient methods for RL that balance between sample complexity, simplicity, and wall-time. The PPO algorithms were tested on benchmark tasks, including simulated robotic locomotion and Atari game playing, outperforming other online policy gradient methods.

4.2 Environments

The ALE introduced by Bellemare et al. (2013) is a platform for evaluating artificial intelligence agents using Atari 2600 game environments. ALE transformed each game into a standard RL problem. It proposed a training and testing methodology for agents, becoming the de facto benchmark for DRL algorithms in discrete action spaces. VizDoom, introduced by Kempka et al. (2016), is a research platform based on the classic first-person shooter game Doom. It allows for developing agents that operate based on visual inputs from the screen buffer and offers highly customisable options. As of 2023, VizDoom is part of the Farama Foundation, a non-profit organisation working to develop and maintain open-source RL tools. OpenAI Gym, developed by Brockman et al. (2016), was a toolkit for developing and comparing RL algorithms. It offered a comprehensive collection of benchmark environments, from simple control tasks to simulated robotic tasks and popular games from the ALE. It quickly became the standardised API for communication between learning algorithms and environments used in most research. Gymnasium (Towers et al., 2023) is an open-source Python evolved from OpenAI’s Gym designed for developing and comparing RL algorithms. Gymnasium is currently maintained by the Farma Foundation and is the official replacement of the discontinued OpenAI Gym, the latter not receiving any future updates or bug fixes. de Lazcano et al. (2023) is a version of Gymnasium for RL in robotic environments. The Minigrid and Miniworld libraries, introduced by Chevalier-Boisvert et al. (2023), are libraries for RL in goal-oriented tasks. These environments are structured as partially observable MDPs and have been used in research for safe RL, curiosity-driven exploration, and meta-learning. Terry et al. (2021) introduced the PettingZoo library, an extension

to Gymnasium designed to facilitate research of Multi-Agent Reinforcement Learning (MARL) algorithms. The library operates based on a novel Agent Environment Cycle games model to make MARL research more accessible and reproducible.

4.3 Physics Object Manipulation

Zhong et al. (2013) presents a method for enhancing the efficiency of Model Predictive Control (MPC) in solving optimal control problems, particularly in high-dimensional systems. The authors propose two strategies to derive a descriptive final cost function to aid MPC in policy selection without extensive future planning or meticulous tuning of cost functions. The first strategy leverages the substantial data generated during MPC simulations to learn the global optimal value function offline for use as a final cost. The second strategy directly solves the Bellman equation using aggregation methods for linearly-solvable MDPs (LMDPs) to approximate the value function and the optimal policy. When integrated into the MPC framework, this approach maintained controller performance quality even with a significantly shortened horizon, demonstrating its potential in real applications. Bejjani et al. (2018) presented a method for real-time manipulation in cluttered environments using a Receding Horizon Planner integrated with a learned value function. The approach interleaves planning and execution in a closed-loop system to dynamically respond to changes during task execution, addressing the challenges posed by the uncertainty in modelling real-world physics. Building on this, Bejjani et al. (2019) integrated end-to-end RL and planning-based look-ahead to real-world manipulation tasks. The research leverages model-free DRL to train a CNN and DNN (CNN+DNN) that map visual observations to actions, one for pushing and the other for grasping, all using a Q-learning framework. The system demonstrated improved grasping success rates and efficiencies in picking experiments. A separate study by Zeng et al. (2018) also explored the synergies between non-prehensile (pushing) and prehensile (grasping) actions in robotic manipulation. The authors used model-free DRL to train two fully convolutional networks (FCNs) that map from visual observations to actions, one for pushing and the other for grasping, in a Q-learning framework. The networks were self-supervised through trial and error, with rewards given for successful grasps, enabling the policy to learn pushing motions that facilitate future grasps and vice versa. A paper by Song et al. (2020) addresses the planar non-prehensile sorting task where a robot must sort densely packed objects of different classes into distinct homogeneous clusters, optionally navigating around immovable ob-

CHAPTER 4. RELATED WORK

stacles. The task is solved using a MCTS algorithm, which is well-suited for high-dimensional state spaces and does not require explicit target states, utilising a discriminative function to identify goal states based on the relative positions of objects.

Chapter 5

Methodology

5.1 Environment

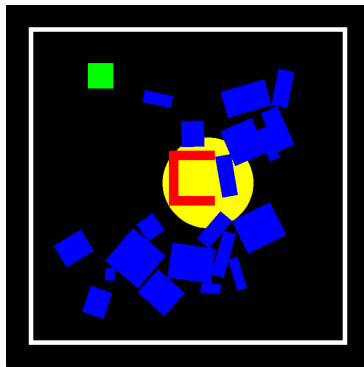


Figure 5.1: An initial state of BGE. Pictured in blue is the clutter, the green square is the goal object, and the yellow circle is the target position.

BGE is a custom environment that is compliant to the v0.26.2 version of the Gymnasium API standard for RL (Towers et al., 2023). The environment simulates a task-oriented scenario where a robotic gripper is manoeuvred to move a goal object to a target goal location. This simulation occurs in a two-dimensional space delineated by predefined borders and uses Pymunk to simulate 2D physics (Blomqvist, 2023). The task is episodic (section 2.1.5 on page 11), and every episode ends in either success, failure or *truncation*. Failure conditions include the gripper or any other object going out of bounds, whereas success is achieved when the goal object is moved onto the target position. Truncation occurs when the episode terminates in neither success nor failure but because the episode takes too long and surpasses a predefined timestep limit. fig. 5.1 graphically represents the environment.

The action space (section 2.1.8 on page 12) is discrete and consists of four possible actions the agent can take at each step: move forward, move backwards, turn left and turn right. The observation space is defined as a raw 800×800 RGB image that represents the current simulator environment state, but changes described in section 5.2 are made such that the final agent observation is a $12 \times 84 \times 84$ vector of luminescence values.

The environment parameters are listed in table 5.4. The *seed* instantiates the numpy random generator (Harris et al., 2020) and is used for reproducibility. *grayscale* and *transpose* enable their respective observation preprocessing steps. *noops* is the number of frames executed at every environment reset before the agent can take action. This is used to both allow the physic objects to come to rest after initial spawn and to populate the starting observation with the stacked frames. *randomise* enables random spawn positions and angles for clutter objects, goal object, target position and gripper agent. *randomise_domain* enables full domain randomisation as described in section 5.3.4. *agent_history_len* controls the number of stacked frames used for observations. *agent_act_repeat* controls the amount of "frame-skipping", meaning that the agent only takes action at intervals defined by *agent_act_repeat*, repeating the last action in the skipped frames. The simulation and physics simulation operate at a rate of 50 Frames Per Second, yielding an effective agent decision rate of $\frac{50}{\text{agent_act_repeat}}$ FPS. This speeds up learning as the agent would otherwise have to make 50 action selections per second. Mnih et al. (2015) had a decision rate of around 15 FPS. *clutter_items* and *clutter_mass* define the number of clutter objects and the weight used for physics calculation. *reward_func* describes the reward evaluation function used to describe the agent goal 2.1.3, and the possible functions are described in detail in 5.3. *max_timesteps* defines an upper bound on the maximum timesteps the agent can use to complete the task. This truncates episodes where the agent is "stuck", and nothing useful would be learnt. *friction_coeff* sets the ground friction coefficient for all object physics calculations.

5.1.1 Agent-environment Interaction as an MDP

We consider tasks where an agent interacts with BGE, a process delineated in section 2.1.6 on page 11. At each timestep, the agent chooses an action from the available actions $\mathcal{A} = \{\text{left, right, forward, backward}\}$. This chosen action is passed to the simulator and influences its internal state, which can also vary randomly due to the environment's stochastic nature. The agent does not observe the internal state. Instead, it observes an image denoted by $X_t \in \mathbb{R}^d$ that represents the current screen in terms of pixel values. Alongside, it

receives a reward signal, noted as R_t , which represents the overarching goal. It is important to note that this reward signal could be influenced by the entire history of actions and observations up to that point; feedback on a particular action might be *delayed* by a substantial number of timesteps. Since the agent only sees the current screen, the environment is partially observable, and the agent can't fully grasp the existing circumstances from the image X_t alone. This leads to a situation where many simulator states are perceptually aliased. To counteract this, we feed sequences of actions and observations $(S_t \sim X_0, A_0, X_1, A_1, \dots, A_{t-1}, X_t)$ as input to the agent to facilitate learning strategies that take into account these series of inputs. Since all sequences are assumed to terminate in a finite number of timesteps, we create a large but finite MDP, wherein each unique sequence represents a distinct state. Therefore, we can apply standard reinforcement learning methods for MDPs described in chapter 3 on page 19 by utilising the full series S_t as the state representation at each timestep t . The agent's goal is to interact with the simulator by selecting actions to maximise future rewards and, by doing so, completing the goal.

5.2 Observation Preprocessing

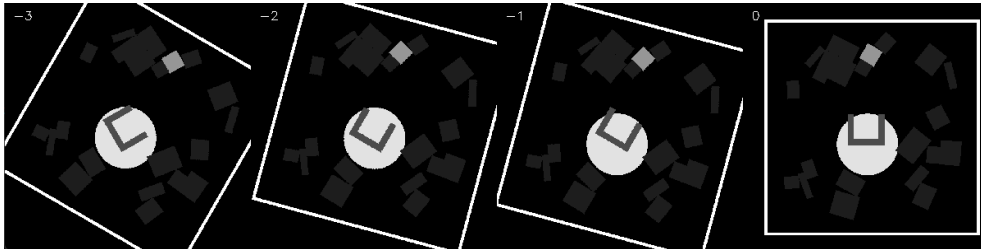


Figure 5.2: Preprocessed and stacked frames forming the agent observation. The frames are ordered right to left, with the most recent frame being the rightmost one.

We first re-centre and rotate the input frame onto the gripper to obtain an *agent-centric view* of the environment, meaning that the image tracks the robot from a top-view perspective. Bejjani (2021) shows that this step significantly improves learning because it enables the agent to take advantage of the symmetries of the scene when compared to a fixed view. We then follow similar preprocessing steps to Mnih et al. (2013), Mnih et al. (2015), which have been shown to facilitate learning and processing at the expense of some visual fidelity. Essential structures and patterns in the image are largely

preserved. First, we *downsample* the high-resolution $3 \times 800 \times 800$ RGB input frame into a lower-resolution $3 \times 84 \times 84$ RGB output frame. We use a function that utilises a nearest-neighbour interpolation technique, which is computationally efficient but might introduce aliasing artefacts due to the omission of result sampling. We then *grayscale* the RGB observation by collapsing the colour information into a single channel. To do so, we extract the Y channel, also known as luminance, from the RGB frame by combining the different colour channels with appropriate weights:

$$Y \leftarrow 0.299R + 0.0587G + 0.114B.$$

resulting in a frame with dimensions $1 \times 84 \times 84$. This still image would not be sufficient to determine the environment’s full dynamics, including the velocities and directions of moving objects. To alleviate this problem, we frame stack the last four frames and use that as the agent observation. We make the observation more Markovian by incorporating some temporal information over a short period. The final dimensions are $4 \times 84 \times 84$. The result of all the preprocessing steps is shown in section 5.2. Before feeding the observation into the neural network, we also normalise the luminescence values to fall within the $[0, 1]$ range.

5.3 Goal Formulation and Evaluation Metrics

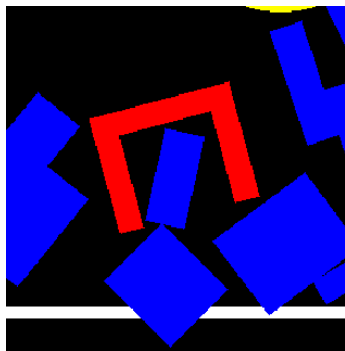


Figure 5.3: The agent pushes a clutter object past the boundary lines, failing the episode.

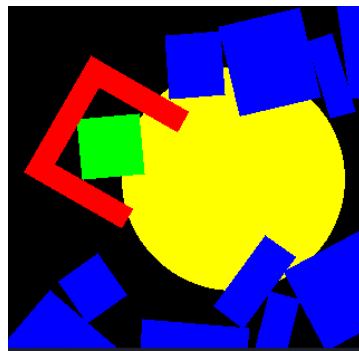


Figure 5.4: The agent successfully pushes the goal object onto the goal position.

We formulate the goal of our task by defining our reward function (see section 2.1.3 on page 10). The agent’s goal should be to grasp the goal object and move it to the target position. We define as *success* the states in which

the goal object is positioned on the target position, as in fig. 5.4. We define *failure* the states in which any object is outside the world boundaries, as in fig. 5.3. We craft a diverse set of reward functions to achieve the goal:

5.3.1 Binary Sparse Rewards

This reward function is a classic reward signal that emits 1 whenever the goal is accomplished, -1 when the task is failed and 0 otherwise:

$$r(s, a, s') = \begin{cases} 1 & \text{if } s' \in \mathbf{success} \\ -1 & \text{if } s' \in \mathbf{failure} \\ 0 & \text{otherwise} \end{cases} \quad (5.1)$$

In RL, binary sparse rewards pose a significant challenge since the only measure of the agent’s efficacy is the anticipated return. Sparse rewards do not guide the agent sufficiently, potentially preventing it from reaching states associated with positive rewards. Consequently, the agent might not improve performance, lacking a clear understanding of its objective.

5.3.2 Reward Shaping

Reward shaping refers to the technique where we incorporate domain knowledge into the reward signal to make the RL algorithms converge more quickly. In this case, we generally aim to reduce the distance between the agent and the goal object and between the goal object and the target position. We can incorporate this information (the domain knowledge) into our reward function to better guide our agent. We can also give a negative base reward at every timestep to encourage the agent to complete the task more quickly.

We define the following notation, where the numbers in the parenthesis are the default values:

r_{fail} : the reward returned upon failure (100).

r_{success} : the reward returned upon success (-100).

d_{gt} : distance from gripper to target.

d_{gtt} : distance from goal to target.

$d_{\text{gt}}^{\text{prev}}$: previous distance from gripper to target.

$d_{\text{gtt}}^{\text{prev}}$: previous distance from goal to target.

$d_{\text{gt}}^{\text{init}}$: the initial distance from gripper to target.

$d_{\text{gtt}}^{\text{init}}$: the initial distance from goal to target.

$d_{\text{total}} = d_{\text{gt}} + d_{\text{gtt}}$

$d_{\text{total}}^{\text{prev}} = d_{\text{gt}}^{\text{prev}} + d_{\text{gtt}}^{\text{prev}}$

$d_{\text{total}}^{\text{init}} = d_{\text{gt}}^{\text{init}} + d_{\text{gtt}}^{\text{init}}$

whereby *previous distance*, we mean the distances computed at the last timestep unless otherwise specified, and by *initial distance*, we mean the distances calculated at the beginning of the episode.

Shaped Reward 1

Here, we give a simple positive reward if the total distance decreases.

$$r(s, a, s') = \begin{cases} r_{\text{fail}} & \text{if } s' \in \text{success} \\ r_{\text{success}} & \text{if } s' \in \text{failure} \\ 2 & \text{if } d_{\text{gt}} < d_{\text{gt}}^{\text{prev}} \text{ and } d_{\text{gtt}} < d_{\text{gtt}}^{\text{prev}} \\ 1 & \text{if } d_{\text{gt}} < d_{\text{gt}}^{\text{prev}} \text{ or } d_{\text{gtt}} < d_{\text{gtt}}^{\text{prev}} \\ -1 & \text{otherwise} \end{cases} \quad (5.2)$$

Shaped Reward 2

Here, we use a predefined budget spread over the entire distance the agent has to close. In this function, the *previous* distances save the shortest distances the agent has ever reached, meaning that the agent will not get a new reward by increasing and then decreasing the distances. We give a budget of $r_{\text{budget}} = 100$.

$$r(s, a, s') = \begin{cases} r_{\text{fail}} & \text{if } s' \in \text{success} \\ r_{\text{success}} & \text{if } s' \in \text{failure} \\ (d_{\text{total}}^{\text{prev}} - d_{\text{total}}) \cdot \frac{r_{\text{budget}}}{d_{\text{total}}^{\text{init}}} & \text{if } d_{\text{total}} < d_{\text{total}}^{\text{prev}} \\ 0 & \text{otherwise} \end{cases} \quad (5.3)$$

Shaped Reward 3

We now define a complex reward clipped into the $\in [-1, 1]$ range. We first define $w_{\text{gt}} = 0.15$, the weight for the distance from gripper to target and $w_{\text{gtt}} = 0.15$, the weight for the distance from goal to target.

$$r(s, a, s') = \begin{cases} r_{\text{fail}} & s' \in \text{success} \\ r_{\text{success}} & \text{if } s' \in \text{failure} \\ r_{\text{computed}} & \text{otherwise} \end{cases} \quad (5.4)$$

$r_{\text{computed}} = \text{clip} \left(2 \cdot \left(\frac{r - r_{\text{min}}}{r_{\text{max}} - r_{\text{min}}} \right), -1, 1 \right)$ where r is defined below as:

$$r = -0.33 - 0.5 \cdot \text{notmoving} + w_{\text{gt}}(d_{\text{gt}}^{\text{best prev}} - d_{\text{gt}}) + w_{\text{gtt}}(d_{\text{gtt}}^{\text{best prev}} - d_{\text{gtt}})$$

Where *notmoving* is a variable that increments each time the gripper and goal remain stationary and resets to zero otherwise.

5.3.3 Curriculum Learning

In *curriculum learning*, we start with a simplified version of the original task and gradually scale back to the standard settings as the agent performance improves. Here, we implement curriculum learning by reducing the initial spawn radius of the goal object and target position and making them closer to the agent. We also steadily increase the number of clutter objects, starting with only a few. Curriculum learning can be used in conjunction with reward shaping.

5.3.4 Domain Randomisation

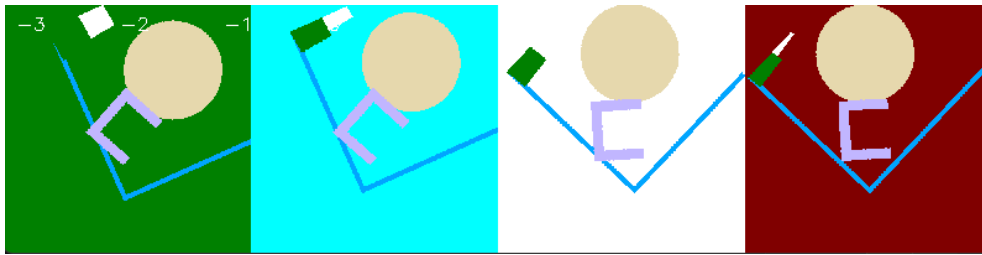


Figure 5.5: Frames with different colours and environment parameters.

By *domain randomisation*, we refer to a technique used to improve the generalization of a trained model to new, unseen environments. This is done by randomly varying aspects of the training environment, such as visual, physical, and even geometrical properties. Here, we use domain randomisation in several manners, including having random initial arrangements for every episode, randomising the number and size of clutter objects, changing up the colours of the environment and varying the world friction coefficient as shown in section 5.3.4. This should, in theory, make our models more resilient to potential noise and avoid overfitting.

5.3.5 Evaluation Metrics

In our agent evaluations, we use two sets of metrics based on the environment type: dynamic and static. For dynamic environments, where elements can change with every reset, we use metrics from 10 separate evaluation environments. We collect data every 10,000 timesteps to create the following charts:

1. **Evaluation mean reward over time:** This is the mean episodic evaluation reward, averaged over 10 episodes. The shaded areas in the

chart show the standard deviation.

2. **Evaluation mean episode length over time:** This chart shows the average episodic evaluation length, found by averaging over 10 episodes.
3. **Evaluation success rate over time:** This is the ratio of successful evaluation episodes to the total number of evaluation episodes, in this case, 10.
4. **Evaluation efficiency over time:** This metric is the mean episodic evaluation reward divided by the mean episodic evaluation length, both averaged over 10 episodes.

We also present tables that list the average episodic reward, average episodic length, and average efficiency at the final training checkpoint. These numbers are averaged over 100 episodes. In all charts and tables, we include a random agent as a *BASELINE*, using statistics averaged over 100 episodes. All charts use a smoothing window of 2 to present the data clearly.

We use metrics from training rollouts for static environments, where everything is fixed and deterministic. Separate evaluation rollouts would show no difference and would be a waste of computational resources. We provide the following plots:

1. **Training reward over time:** This shows the mean episodic training reward averaged over 100 episodes and the number of environment timesteps.
2. **Training episode length over time:** This chart shows the mean episodic training length, averaged over 100 episodes and the number of timesteps.
3. **Training efficiency over time:** This is calculated as the mean episodic training reward divided by the mean episodic length, both averaging over 100 episodes.

We also present tables listing the average episodic reward, average episodic length, and average efficiency at the last training checkpoint for a single deterministic episode.

5.4 Agent Architecture

The overall agent architecture varies depending on the algorithms used, but we use the same feature extraction CNN layers across all architectures. The

input to the neural network consists of a $4 \times 84 \times 84$ image produced by the preprocessing, which is then processed as follows:

- Convolutional Layer 1: 32 filters, kernel size 8×8 , stride 4, followed by ReLU activation (rectifier nonlinearity). Input size is $12 \times 84 \times 84$, output size is $32 \times 20 \times 20$.
- Convolutional Layer 2: 64 filters, kernel size 4×4 , stride 2, followed by ReLU activation. The input size is $32 \times 20 \times 20$, and the output size is $64 \times 9 \times 9$.
- Convolutional Layer 3: 64 filters, kernel size 3×3 , stride 1, followed by ReLU activation. Input size is $64 \times 9 \times 9$, output size is $64 \times 7 \times 7$, flattened to 3136.

Figures figs. 5.6 and 5.7 show max-pooling layers equivalent to the strides listed here. We use PyTorch to build the DNNs (Paszke et al., 2019).

5.4.1 Deep Q-Network Architecture

The DQN agent architectures have an additional final hidden layer of 512 fully connected rectifier units in addition to the layers listed in section 5.4. The output layer is a fully connected linear layer with a single output for each of the 4 valid actions, where the final action is selected according to an ϵ -greedy policy. As described in algorithm 4 on page 31, DQN uses a copy of the Q-network to stabilise training. We use two copies of the full DNN shown in fig. 5.6.

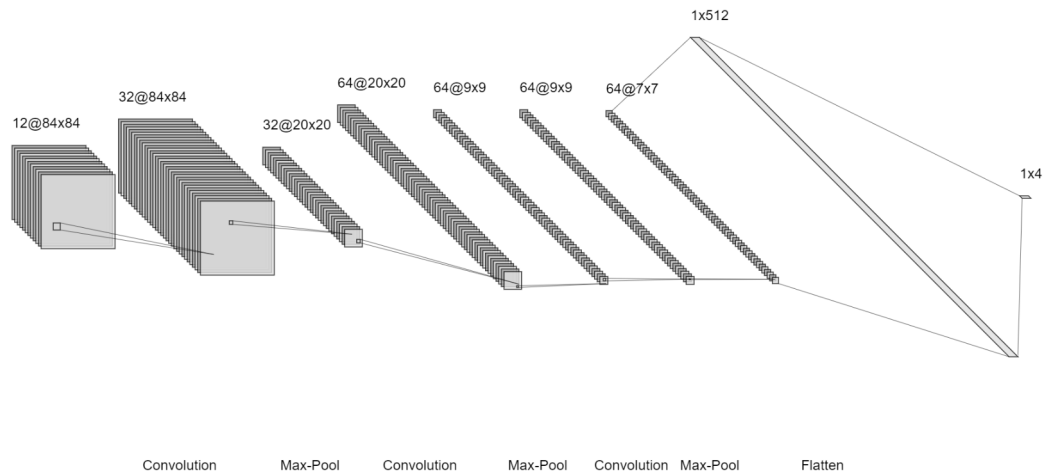


Figure 5.6: Network architecture for DQN. A CNN is used for featured extraction and is followed by a hidden, fully connected layer.

5.4.2 Actor-Critic Architecture

We use the same actor-critic architecture for both PPO and A2C. We feed the outputs of the convolutional layers described in section 5.4 to two different fully connected layers of 512 rectifier hidden units each, one for the actor and one for the critic. The actor connects the fully connected layer to an output layer of 4 units, one for each action, and the action is then selected using softmax. The critic connects the fully connected layer to a single output unit representing the value of the state. The architecture is shown schematically in fig. 5.7, and its motivation is discussed in section 3.4 on page 35.

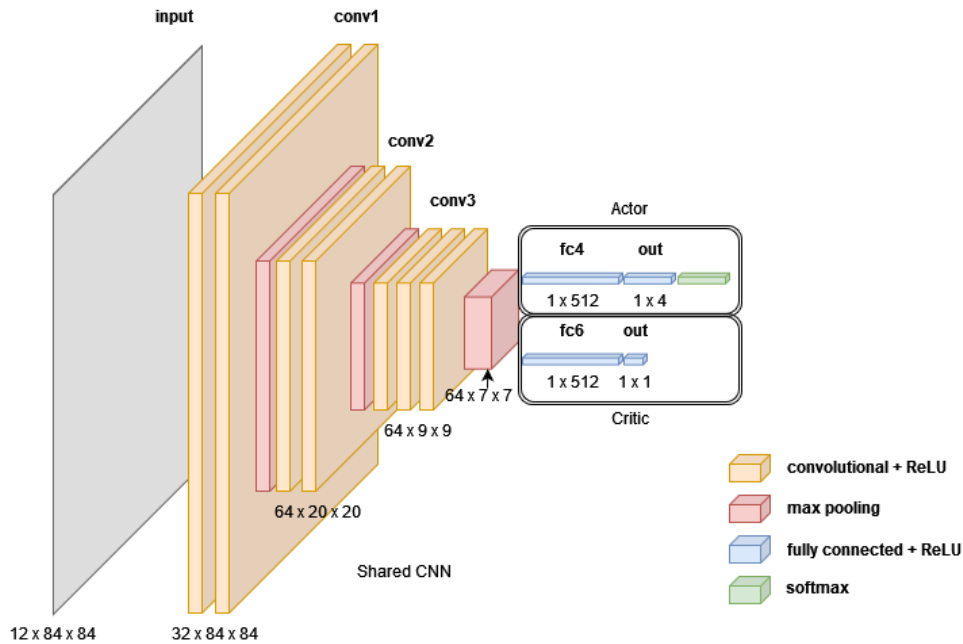


Figure 5.7: Actor-critic network architecture used for both PPO and A2C. A CNN is shared between the actor and critic for featured extraction, followed by separate fully connected layers for the actor and the critic.

5.5 Training and Evaluation

For each experiment in 6, we train our agents for 2 Million timesteps. Algorithm-specific training information is logged and monitored through Tensorboard, including metrics such as the learning rate, value loss, policy gradient loss, and current entropy coefficient. The models are evaluated every 10000 timesteps with 5 evaluation environments where the mean episode length, mean episodic reward and success rate are recorded and saved. The primary evaluation metric remains the mean episodic training reward, averaging over 100 episodes. The mean episodic length, averaged over 100 episodes, determines the agent’s efficiency. We retrain a different network for each experiment for every algorithm, but we keep the same hyperparameters to test for generalisation. Example training code is given in algorithm 10.

Algorithm 10 Example code for training an agent on BGE

```
1: procedure TRAINAGENT(max_episodes)
2:   env  $\leftarrow$  initialise the environment
3:   agent  $\leftarrow$  AGENT.INIT(env.observation_space, env.action_space)
4:   episode  $\leftarrow$  0
5:   while episode < max_episodes do
6:     state  $\leftarrow$  env.RESET
7:     episodic_reward  $\leftarrow$  0
8:     terminated  $\leftarrow$  False
9:     while not terminated do
10:      action  $\leftarrow$  agent.SELECTACTION(state)
11:      next_state, reward, terminated, info  $\leftarrow$  env.STEP(action)
12:      agent.STORETRANSITION(state, action, reward, next_state, done)
13:      agent.OPTIMIZEMODEL
14:      state  $\leftarrow$  next_state
15:      total_reward  $\leftarrow$  total_reward + reward
16:     print "Episode: ", episode, "Total Reward: ", total_reward
17:     episode  $\leftarrow$  episode + 1
```

5.5.1 Algorithms and Environment Parameters

We give tables for the hyperparameters used for all experiments. A non-exhaustive hyperparameter search was conducted using Optuna (Akiba et al., 2019). For details about how the hyperparameters affect their respective algorithms, see DQN in section 3.2.4 on page 29, A2C in section 3.4.1 on page 36 and PPO in section 3.4.2 on page 37.

Table 5.1: DQN Hyperparameters

Parameter	Value	Description
learning_rate	1×10^{-4}	Learning rate
buffer_size	1,000,000	Size of the replay buffer
learning_starts	50,000	Steps before learning starts
batch_size	32	Minibatch size for gradient update
gamma	0.99	Discount factor
train_freq	4	Training frequency
gradient_steps	1 or -1	Number of gradient steps after each rollout
target_update_interval	10,000	Target network update interval
exploration_fraction	0.1	Fraction of training period for exploration
exploration_initial_eps	1.0	Initial exploration probability
exploration_final_eps	0.05	Final exploration probability
max_grad_norm	10	Maximum gradient clipping value

Table 5.2: PPO Hyperparameters

Parameter	Value	Description
learning_rate	3×10^{-4}	Learning rate
n_steps	2048	Number of steps per update
batch_size	64	Minibatch size
n_epochs	10	Number of epochs for loss optimization
gamma	0.99	Discount factor
gae_lambda	0.95	GAE trade-off factor
clip_range	0.2	Clipping parameter
clip_range_vf	None	Value function clipping parameter
normalize_advantage	True	Normalize advantage or not
ent_coef	0.0	Entropy coefficient
vf_coef	0.5	Value function coefficient
max_grad_norm	0.5	Maximum gradient clipping value

Table 5.3: A2C Hyperparameters

Parameter	Value	Description
learning_rate	7×10^{-4}	Learning rate
n_steps	5	Number of steps per update
gamma	0.99	Discount factor
gae_lambda	1.0	GAE trade-off factor
ent_coef	0.0	Entropy coefficient
vf_coef	0.5	Value function coefficient
max_grad_norm	0.5	Maximum gradient clipping value
rms_prop_eps	1×10^{-5}	RMSProp epsilon
normalize_advantage	False	Normalize advantage or not

Table 5.4: Description of environment parameters

Parameter	Type	Brief description
seed	integer	Sets the seed for the environment
grayscale	boolean	Enables grayscale observations
transpose	boolean	Transposes the observation onto the gripper point of view
noops	integer	Number of noops executed on environment reset
randomise	boolean	Enables spawn positions randomisation
randomise_domain	boolean	Enables full domain randomisation
agent_history_len	integer	Number of stacked frames
agent_act_repeat	integer	Controls the agent decision rate
agent_speed	float	Agent speed
agent_ang_speed	float	Agent angular speed
clutter_items	integer	Number of clutter items
clutter_mass	float	Mass of the clutter objects
reward_func	callable	Specifies the reward evaluation function
max_timesteps	integer	Maximum timesteps before the environment is truncated
friction_coeff	float	Ground friction coefficient

Chapter 6

Experiments

In this chapter, we will show experiments whose results are meaningful and add value to the discussion. Many other preliminary experiments have been conducted and discarded, often yielding predictable and uninteresting results. In chapter 6, we give the default environment parameters, which will be used in the experiments unless explicitly stated otherwise.

Table 6.1: Global Environment Parameters

Parameter	Default Value
grayscale	True
transpose	True
noops	50
randomise	True
randomise_domain	False
agent_history_len	4
agent_act_repeat	4
agent_speed	300
agent_ang_speed	4.91
clutter_items	10
clutter_mass	1.0
max_timesteps	300
friction_coeff	0.2

6.1 Experiment I

In this experiment, we use the static environment setup and the sparse reward function shown in section 5.3.1 on page 49.

Table 6.2: Environment Parameters

Parameter	Value
seed	756765
randomise	False
clutter_items	1

Table 6.3: Baseline Performance

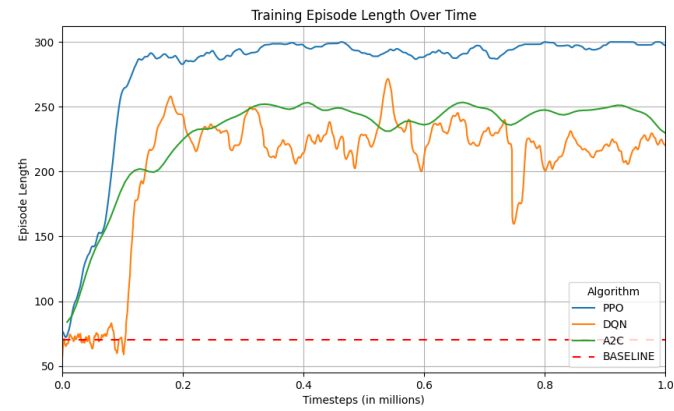
Metric	Value
Mean Reward	-0.98 \pm 0.14
Mean Length	70.20
Mean Efficiency	-0.014
Success Rate	0.01

Table 6.4: Final Performance

Metric	PPO	A2C	DQN	DQN
Timesteps	1,000,000	1,000,000	1,000,000	900,000
Reward	0.00	0.00	-1.00	0.00
Length	300	300	28	300
Efficiency	0	0	-0.04	0
Success Rate	0	0	0	0



(a) Training reward over time.



(b) Training episode length over time.



(c) Training efficiency over time.

Figure 6.1: Agent performance in experiment I.

6.1.1 Results

The graphs in the graphs in fig. 6.1 show that the agent fails to learn how to solve the task, as they never get to see the positive reward for successful completion. In the final models shown in 6.4, PPO learns to rotate in place until the episode terminates continuously, and A2C has a similar behaviour. The DQN agent fails the task at the latest checkpoint but behaves similarly to the other at 900000 timesteps. The agents all perform better than the baseline.

6.2 Experiment II

In this experiment, we use the static environment setup and seed of section 6.1 but use the naive dense reward function shown in eq. (5.2) on page 50.

Table 6.5: Environment Parameters

Parameter	Value
seed	756765
randomise	False
clutter_items	1

Table 6.6: Baseline Performance

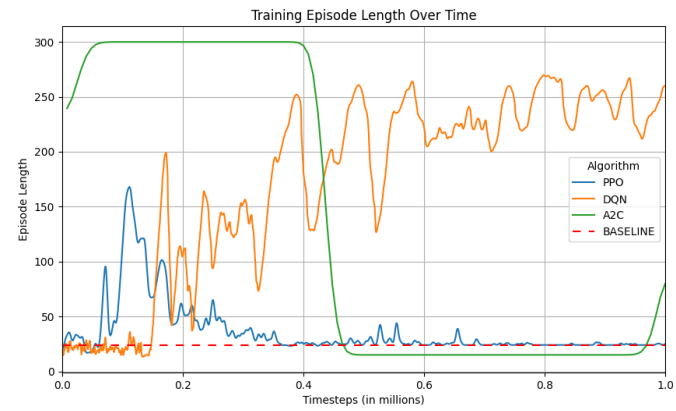
Metric	Value
Mean Reward	-88.62 \pm 31.85
Mean Length	23.68
Mean Efficiency	-3.74
Success Rate	0.00

Table 6.7: Final Performance

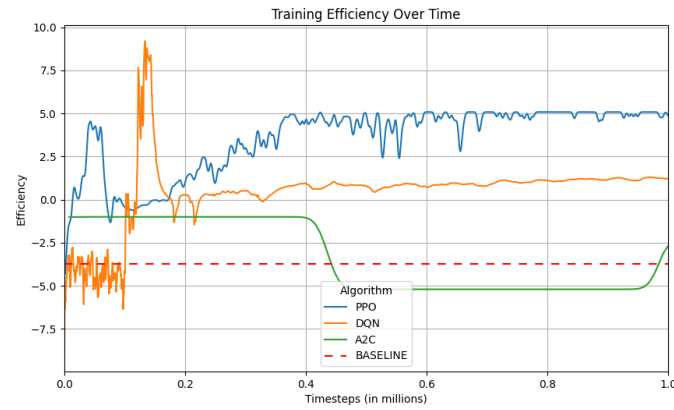
Metric	PPO	A2C	DQN
Timesteps	1,000,000	1,000,000	1,000,000
Reward	122.0	-78.0	404.0
Length	24	15	30
Efficiency	5.08	-5.2	13.47
Success Rate	1	0	0



(a) Training reward over time.



(b) Training episode length over time.



(c) Training efficiency over time.

Figure 6.2: Agent performance in experiment II.

6.2.1 Results

Looking at the charts in fig. 6.2, it appears DQN performs best. However, that is not the case. table 6.7 shows how despite achieving 404 of mean episodic reward, its success rate is 0. This is because the agent has learnt to exploit our naive reward function and keeps moving back and forth to accumulate reward instead of completing the real goal. On the other hand, PPO, who initially appears to have lower performance, actually learned to solve the task. A2C behaves similarly to experiment I.

6.3 Experiment III

We start examining fully randomised environments. We use the budgeted reward function defined in eq. (5.3) on page 50.

Table 6.8: Environment Parameters

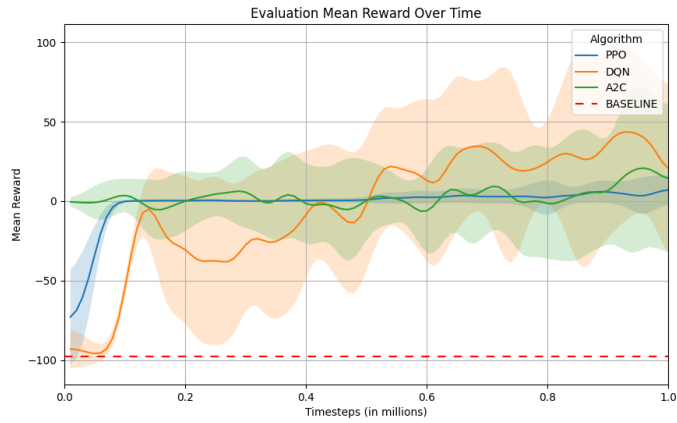
Parameter	Value
seed	934612
randomise	True
clutter_items	3

Table 6.9: Baseline Performance

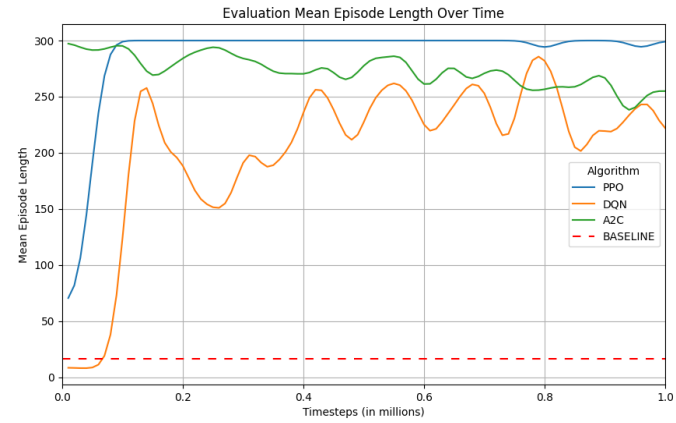
Metric	Value
Mean Reward	-97.82 ± 4.18
Mean Length	16.44
Mean Efficiency	-5.95
Success Rate	0.00

Table 6.10: Final Performance

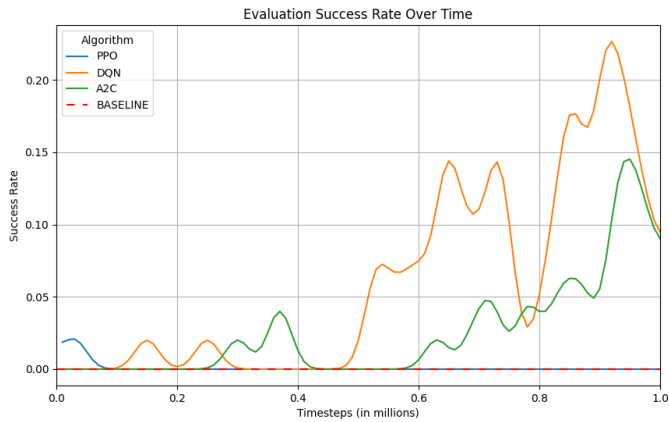
Metric	PPO	A2C	DQN
Timesteps	1,000,000	1,000,000	1,000,000
Mean Reward	6.00 ± 7.93	6.87 ± 7.56	41.43 ± 66.34
Mean Length	300.0 ± 0.0	300.0 ± 0.0	202.62 ± 135.76
Mean Efficiency	0.02	0.02	0.20
Success Rate	0.00	0.00	0.22



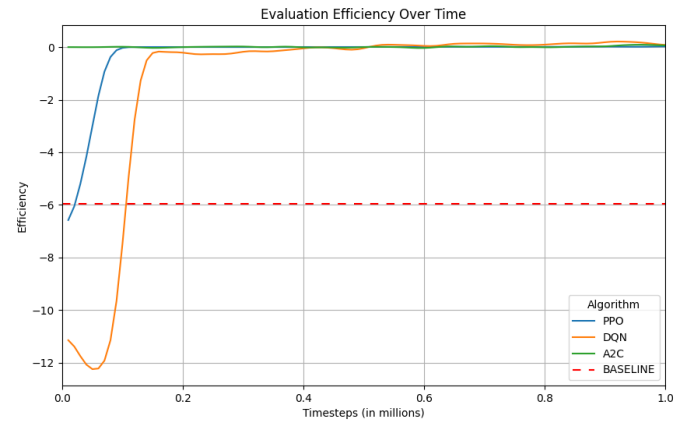
(a) Evaluation mean reward over time.



(b) Evaluation mean episode length over time.



(c) Evaluation success rate over time.



(d) Evaluation efficiency over time.

Figure 6.3: Agent performance in experiment III.

6.3.1 Results

We see from plots in fig. 6.3 that the reward function seems more representative of agent performance this time. PPO and A2C have again converged to the local optimum of rotating in place until episode termination to avoid any negative reward. DQN in table 6.10 only rarely achieves the goal.

6.4 Experiment IV

We try using domain randomisation along with the complex reward function in eq. (5.4) on page 50 to guide the agent.

Table 6.11: Environment Parameters

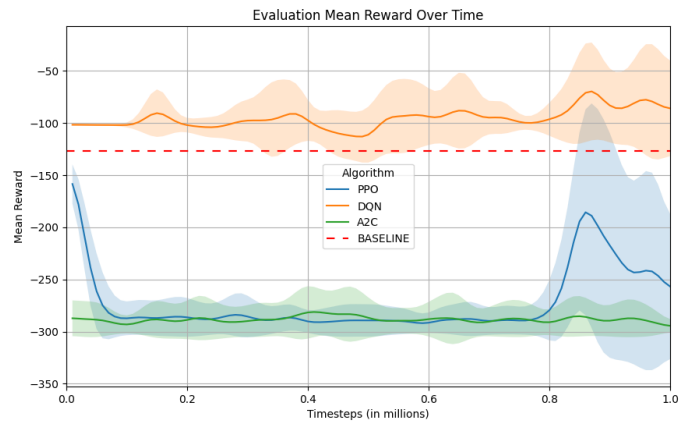
Parameter	Value
seed	467328
randomise	True
randomise_domain	True
clutter_items	3

Table 6.12: Baseline Performance

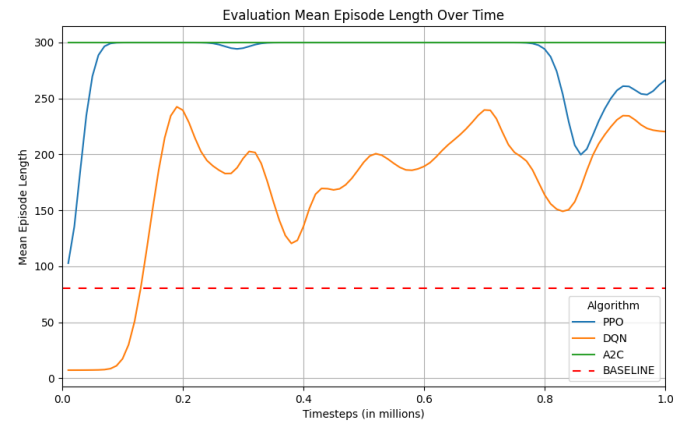
Metric	Value
Mean Reward	-126.55 \pm 23.03
Mean Length	80.12
Mean Efficiency	-1.58
Success Rate	0.00

Table 6.13: Final Performance

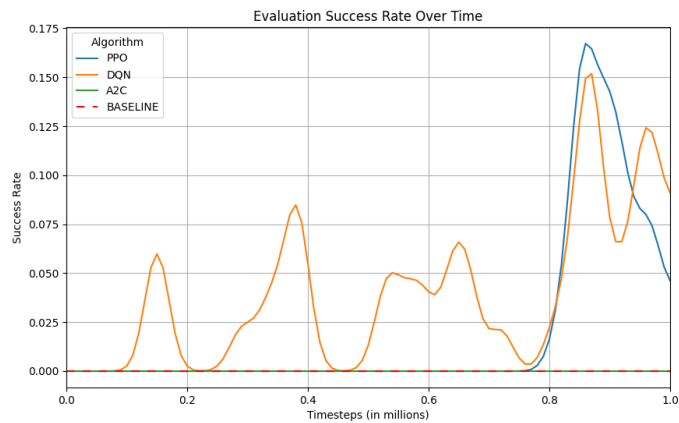
Metric	PPO	A2C	DQN
Timesteps	1,000,000	1,000,000	1,000,000
Mean Reward	-249.27 \pm 94.82	-285.42 \pm 20.32	-92.67 \pm 40.41
Mean Length	261.13 \pm 96.40	300.0 \pm 0.0	180.48 \pm 138.09
Mean Efficiency	-0.95	-0.95	-0.51
Success Rate	0.05	0.0	0.04



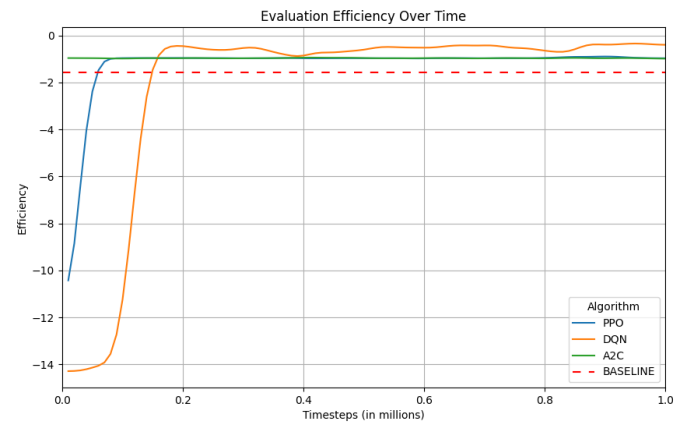
(a) Evaluation mean reward over time.



(b) Evaluation mean episode length over time.



(c) Evaluation success rate over time.



(d) Evaluation efficiency over time.

Figure 6.4: Agent performance in experiment IV.

6.4.1 Results

fig. 6.4 and table 6.13 show that the random baseline performs better than the agents, with DQN only marginally better. This is probably caused by the domain randomisation, making it impossible for the agent to distinguish the goal object from the clutter.

6.5 Experiment V

We revisit section 5.3.1 on page 49 with a slight modification. At every timestep, the reward is -1 instead of 0 , and $+1$ for successfully completing the episode.

Table 6.14: Environment Parameters

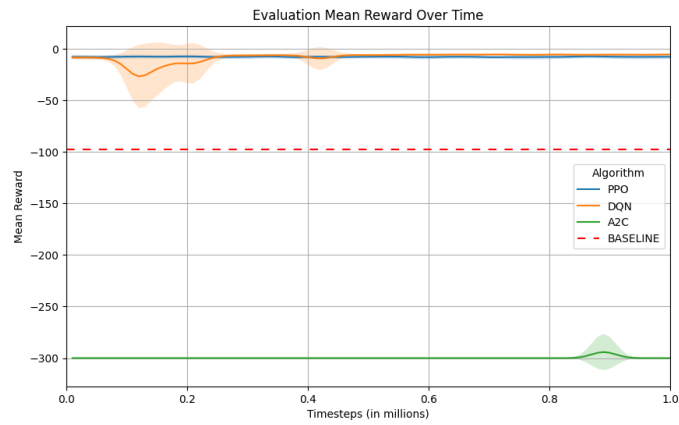
Parameter	Value
seed	115545
randomise	True
clutter_items	1

Table 6.15: Baseline Performance

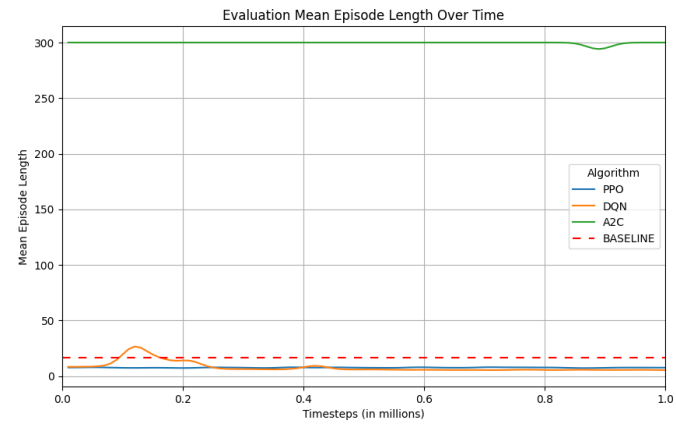
Metric	Value
Mean Reward	-90.36 ± 69.73
Mean Length	90.36
Mean Efficiency	-1.0
Success Rate	0.0

Table 6.16: Final Performance

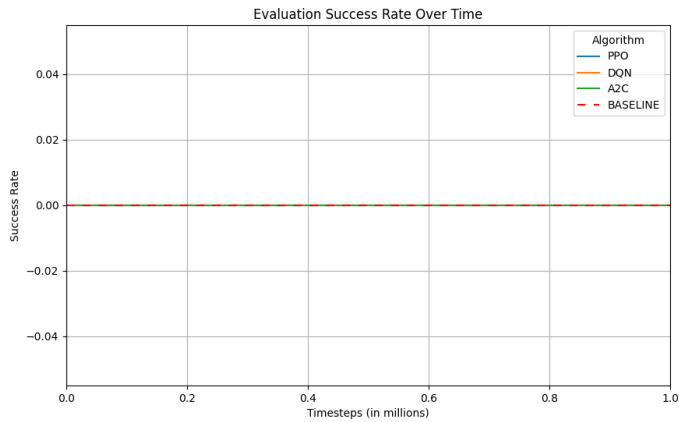
Metric	PPO	A2C	DQN
Timesteps	1,000,000	1,000,000	1,000,000
Mean Reward	-8.3 ± 1.82	-300.0 ± 0.0	-5.89 ± 1.84
Mean Length	8.3 ± 1.82	300.0 ± 0.0	5.89 ± 1.84
Mean Efficiency	-1.0	-1.0	-1.0
Success Rate	0.0	0.0	0.0



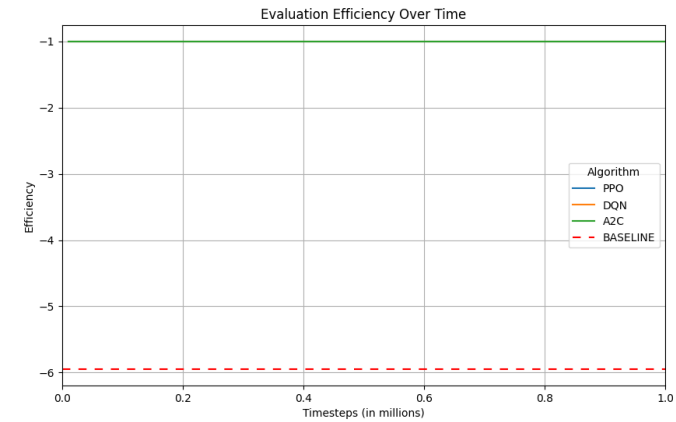
(a) Evaluation mean reward over time.



(b) Evaluation mean episode length over time.



(c) Evaluation success rate over time.



(d) Evaluation efficiency over time.

Figure 6.5: Agent performance in experiment V.

6.5.1 Results

fig. 6.5 clearly shows that PPO and DQN have found the same strategy to maximise reward. Once the episode tasks, they find the quickest way to self-destruct, as they predict they would get more negative reward if they attempted any other course of action. A2C rotates around its initial position.

6.6 Experiment VI: Extended Training

We now try training our agents for a longer number of timesteps. We select the more promising algorithms, PPO and DQN, and the reward function in eq. (5.3) on page 50, which seems to represent the goal better. We use curriculum learning in the following way to facilitate training: the environment starts with the goal object spawning near the target position, and we slowly increase the randomness radii upon each successful episode completion. We run the training for a total of 9 million timesteps and we evaluate the agents in fully randomised environments.

Table 6.17: Environment Parameters

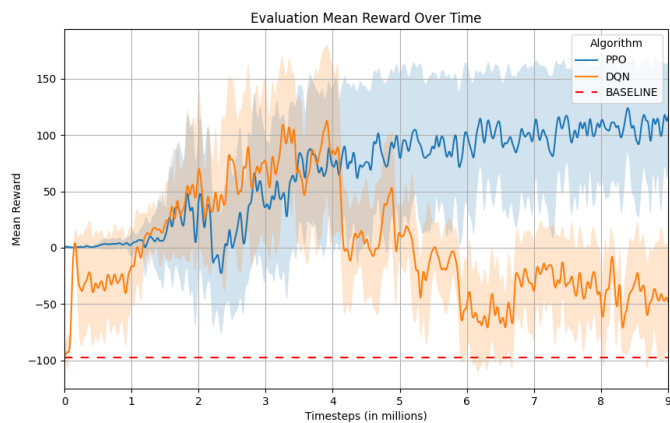
Parameter	Value
seed	433854
randomise	True
clutter_items	3

Table 6.18: Baseline Performance

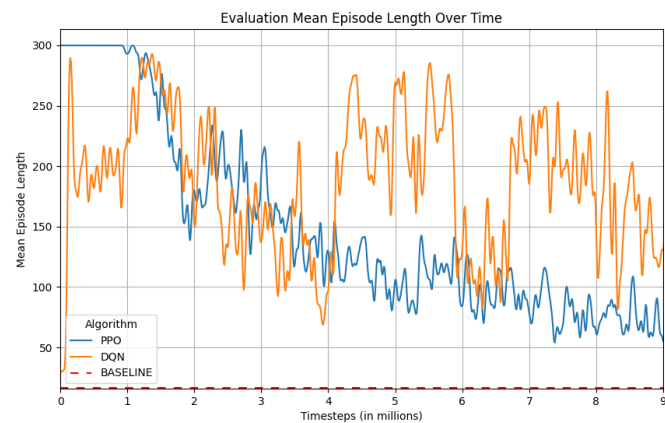
Metric	Value
Mean Reward	-95.07 ± 5.69
Mean Length	99.17
Mean Efficiency	-0.96
Success Rate	0.00

Table 6.19: Final Performance

Metric	PPO	DQN (4mln)	DQN
Timesteps	1,000,000	4,000,000	1,000,000
Mean Reward	100.14 ± 70.83	86.62 ± 81.76	-28.75 ± 53.06
Mean Length	79.9 ± 117.04	103.03 ± 126.22	184.95 ± 140.96
Mean Efficiency	1.25	0.84	-0.16
Success Rate	0.73	0.58	0.01



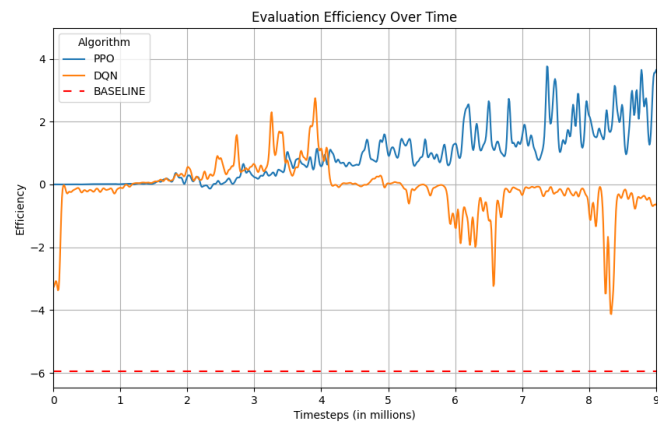
(a) Evaluation mean reward over time.



(b) Evaluation mean episode length over time.



(c) Evaluation success rate over time.



(d) Evaluation efficiency over time.

Figure 6.6: Agent performance in experiment VI.

6.6.1 Results

fig. 6.6 sees a significant drop in performance for DQN around 4 million timesteps. This is a common phenomenon in DQN called *catastrophic forgetting*. Remember that we run DQN with a replay buffer of 1 million transitions, as shown in its hyperparameters table 5.1 on page 57. Once the buffer is full, DQN discards the oldest observations and replaces them with new ones without any prioritisation mechanism. Because of this, it can start overestimating the Q-values of all actions since it has forgotten experiences that lead to failure. Hence, catastrophic forgetting occurs. On the other hand, we see that PPO maintains good performance with a 0.73 success rate. Still, testing shows that transferring the trained PPO model to an environment with 5 clutter objects plummeted the success rate to 0.22. Upon investigation, it appears that the PPO agent refuses to complete the task whenever there is a clutter object between him and the goal object, preferring instead to avoid failure by rotating in place until the truncation of the episode.

Chapter 7

Conclusion and Future Work

7.1 Results Discussion

The results show significant difficulties for all agents in solving the task, even under simplified circumstances. Part of this can be linked to the goal formulation. Using binary sparse rewards settings seems to be the fairest way as it directly rewards the agent for doing what we want. However, this approach didn't work well within the reasonable computational limits we had. Without clear guidance, the agent rarely finds a successful action sequence on its own. This is more pronounced when using the ϵ -greedy exploratory policy, which doesn't maintain a steady exploration strategy. Similarly, policy-gradient methods often get stuck at a local optimum despite using techniques like entropy regularisation to encourage exploration. Using reward shaping is also problematic, often leading to unforeseen consequences. When we defined the goal as moving an object to a specific position, it was hard to do this without influencing the agent's behaviour. Defining the goal of moving an object to a position is difficult to express as a shaped reward signal without imparting bias to the agent. Suppose we define the reward signal in relation to reducing the distance between the agent and the goal, as we have done in most of our experiments. In that case, it will discourage other valid strategies, such as using other objects to push the goal. The experiments have shown that a poorly shaped reward can cause the agent to terminate the scenario without any attempt to solve it. The task we defined here is fundamentally different from the well-studied Atari games. Atari games are deterministic, and the levels have similar sequences of actions to complete the task. During training, stochasticity is artificially introduced in the environment using techniques like random starts or randomly repeated actions. Atari games also have a well-defined, non-sparse reward signal,

namely the underlying game score. A reward increase represents something we want, not some proxy heuristic function for some overarching goal.

7.2 Future Work

There are many ways to build upon this research. In future, we want to explore different methods to give the agent some prior knowledge. According to Sutton and Barto (2018), domain knowledge should be given using not complex reward shaping but direct policy initiation. For instance, Hester et al. (2018) has shown that it is possible to significantly speed up training by using even a few expert demonstrations of successful completion. The training is typically done through standard supervised learning or some other imitation learning method. This technique is particularly effective for the largely deterministic Atari games, where the desired trajectories are somewhat similar to the expert trajectories. Here, similar attempts have yielded no significant change in performance. Bejjani et al. (2021) proposed a more applicable practical approach where a large number of expert trajectories are generated using classic open-loop planning. Adding imitation learning to the training procedure is a potential area to delve into. We also aim to improve existing algorithms. We used a classic DQN version based on Mnih et al. (2015), but many enhancements have been made since then. Using the latest DQN algorithms or trying massively parallel policy-gradient methods could yield better results, as suggested by the extended training experiment. Other improvements could also be made on the feature extraction DNN side: using more modern CNNs architectures that have better feature extraction can lead to significant improvements in generalisation and performance, as shown in Cobbe et al. (2019). Another possible avenue for research would be to use a model-based DRL approach, possibly with learned environment dynamics to predict physics interactions. In addition, here, we have strictly considered a discrete action space. Using a continuous action space makes it possible to utilise DRL algorithms that would be otherwise incompatible.

7.3 Conclusions

This thesis has provided a general overview and introduction to modern Reinforcement Learning, including all the mathematical background needed for three well-established algorithms: Deep Q-Network, Proximal Policy Optimisation and Advantage Actor-Critic. We developed an environment called the Bidimensional Gripper Environment (BGE) that simulates a physics-based

top-down world reminiscent of a table, where a gripper agent has to push a goal object onto a goal position. We have implemented preprocessing steps to make the environment observation more Markovian, and we have made it compatible with a CNN for end-to-end training and automatic feature extraction. We have used the CNN as part of DRL agent architectures and then trained said agents in our environment. We reported the result of six experiments with different combinations of reward function, randomness and clutter obstacles. The inconclusive results show that these Model-free algorithms fail to accomplish the task reliably, especially in a way that would be transferable to real-world systems. Reward shaping has also proven problematic, and our goal formulation as a non-sparse reward signal is unclear. In many cases, the agent preferred to maximise the given heuristic instead of actually completing the task. We concluded by providing recommendations for augmenting our RL algorithms, including a call for better feature-extracting networks, better policy initialisation through imitation learning methods and more advanced or more distributed algorithms.

Bibliography

- Achiam, J. (2018). Spinning up in deep reinforcement learning. Retrieved August 29, 2023, from <https://spinningup.openai.com>
- Akiba, T., Sano, S., Yanase, T., Ohta, T., & Koyama, M. (2019). Optuna: A next-generation hyperparameter optimization framework. *Proceedings of the 25th ACM SIGKDD International Conference on Knowledge Discovery & Data Mining*, 2623–2631. <https://doi.org/10.1145/3292500.3330701>
- Bejjani, W. (2021, January). *Learning deep policies for physics-based robotic manipulation in cluttered real-world environments* [Doctoral dissertation, University of Leeds]. Retrieved June 1, 2023, from <https://etheses.whiterose.ac.uk/28954/>
- Bejjani, W., Dogar, M. R., & Leonetti, M. (2019). Learning physics-based manipulation in clutter: Combining image-based generalization and look-ahead planning [ISSN: 2153-0866]. *2019 IEEE/RSJ International Conference on Intelligent Robots and Systems (IROS)*, 6562–6569. <https://doi.org/10.1109/IROS40897.2019.8967717>
- Bejjani, W., Leonetti, M., & Dogar, M. R. (2021). Learning image-based receding horizon planning for manipulation in clutter. *Robotics and Autonomous Systems*, 138, 103730. <https://doi.org/10.1016/j.robot.2021.103730>
- Bejjani, W., Papallas, R., Leonetti, M., & Dogar, M. R. (2018). Planning with a receding horizon for manipulation in clutter using a learned value function [ISSN: 2164-0580]. *2018 IEEE-RAS 18th International Conference on Humanoid Robots (Humanoids)*, 1–9. <https://doi.org/10.1109/HUMANOIDS.2018.8624977>
- Bellemare, M. G., Naddaf, Y., Veness, J., & Bowling, M. (2013). The arcade learning environment: An evaluation platform for general agents. *Journal of Artificial Intelligence Research*, 47, 253–279. <https://doi.org/10.1613/jair.3912>
- Blomqvist, V. (2023, June). *Pymunk* (Version 6.5.1). Retrieved August 23, 2023, from <https://pymunk.org>

- Brockman, G., Cheung, V., Pettersson, L., Schneider, J., Schulman, J., Tang, J., & Zaremba, W. (2016, June 5). OpenAI gym. <https://doi.org/10.48550/arXiv.1606.01540>
- Brown, T., Mann, B., Ryder, N., Subbiah, M., Kaplan, J. D., Dhariwal, P., Neelakantan, A., Shyam, P., Sastry, G., Askell, A., Agarwal, S., Herbert-Voss, A., Krueger, G., Henighan, T., Child, R., Ramesh, A., Ziegler, D., Wu, J., Winter, C., . . . Amodei, D. (2020). Language models are few-shot learners. *Advances in Neural Information Processing Systems*, *33*, 1877–1901. Retrieved August 25, 2023, from <https://papers.nips.cc/paper/2020/hash/1457c0d6bfcb4967418bfb8ac142f64a-Abstract.html>
- Chevalier-Boisvert, M., Dai, B., Towers, M., de Lazcano, R., Willems, L., Lahlou, S., Pal, S., Castro, P. S., & Terry, J. (2023). Minigrid & miniworld: Modular & customizable reinforcement learning environments for goal-oriented tasks. *CoRR*, *abs/2306.13831*.
- Cobbe, K., Klimov, O., Hesse, C., Kim, T., & Schulman, J. (2019, July 14). Quantifying generalization in reinforcement learning. <https://doi.org/10.48550/arXiv.1812.02341>
- Dalgaard, M., Motzoi, F., Sørensen, J. J., & Sherson, J. (2020). Global optimization of quantum dynamics with AlphaZero deep exploration [Number: 1 Publisher: Nature Publishing Group]. *npj Quantum Information*, *6*(1), 1–9. <https://doi.org/10.1038/s41534-019-0241-0>
- DeepMind. (2020a, March 13). *AlphaGo*. Retrieved August 26, 2023, from <https://www.deepmind.com/research/highlighted-research/alphago>
- DeepMind. (2020b, March 31). *Agent57: Outperforming the human atari benchmark*. Retrieved August 26, 2023, from <https://www.deepmind.com/blog/agent57-outperforming-the-human-atari-benchmark>
- de Lazcano, R., Andreas, K., Tai, J. J., Lee, S. R., & Terry, J. (2023). *Gymnasium robotics* (Version 1.2.0). <http://github.com/Farama-Foundation/Gymnasium-Robotics>
- Fawzi, A., Balog, M., Huang, A., Hubert, T., Romera-Paredes, B., Barekatin, M., Novikov, A., R. Ruiz, F. J., Schrittwieser, J., Swirszcz, G., Silver, D., Hassabis, D., & Kohli, P. (2022). Discovering faster matrix multiplication algorithms with reinforcement learning [Number: 7930 Publisher: Nature Publishing Group]. *Nature*, *610*(7930), 47–53. <https://doi.org/10.1038/s41586-022-05172-4>
- Francois-Lavet, V., Henderson, P., Islam, R., Bellemare, M. G., & Pineau, J. (2018). An introduction to deep reinforcement learning. *Foundations and Trends® in Machine Learning*, *11*(3), 219–354. <https://doi.org/10.1561/22000000071>
- Goodfellow, I., Bengio, Y., & Courville, A. (2016). *Deep learning*. MIT Press.

- Harris, C. R., Millman, K. J., van der Walt, S. J., Gommers, R., Virtanen, P., Cournapeau, D., Wieser, E., Taylor, J., Berg, S., Smith, N. J., Kern, R., Picus, M., Hoyer, S., van Kerkwijk, M. H., Brett, M., Haldane, A., del Río, J. F., Wiebe, M., Peterson, P., . . . Oliphant, T. E. (2020). Array programming with NumPy [Publisher: Springer Science and Business Media LLC]. *Nature*, *585*(7825), 357–362. <https://doi.org/10.1038/s41586-020-2649-2>
- Hessel, M., Modayil, J., Hasselt, H. v., Schaul, T., Ostrovski, G., Dabney, W., Horgan, D., Piot, B., Azar, M., & Silver, D. (2018). Rainbow: Combining improvements in deep reinforcement learning [Number: 1]. *Proceedings of the AAAI Conference on Artificial Intelligence*, *32*(1). <https://doi.org/10.1609/aaai.v32i1.11796>
- Hester, T., Vecerik, M., Pietquin, O., Lanctot, M., Schaul, T., Piot, B., Horgan, D., Quan, J., Sendonaris, A., Osband, I., Dulac-Arnold, G., Agapiou, J., Leibo, J., & Gruslys, A. (2018). Deep q-learning from demonstrations [Number: 1]. *Proceedings of the AAAI Conference on Artificial Intelligence*, *32*(1). <https://doi.org/10.1609/aaai.v32i1.11757>
- Jumper, J., Evans, R., Pritzel, A., Green, T., Figurnov, M., Ronneberger, O., Tunyasuvunakool, K., Bates, R., Žídek, A., Potapenko, A., Bridgland, A., Meyer, C., Kohl, S. A. A., Ballard, A. J., Cowie, A., Romera-Paredes, B., Nikolov, S., Jain, R., Adler, J., . . . Hassabis, D. (2021). Highly accurate protein structure prediction with AlphaFold [Number: 7873 Publisher: Nature Publishing Group]. *Nature*, *596*(7873), 583–589. <https://doi.org/10.1038/s41586-021-03819-2>
- Kempka, M., Wydmuch, M., Runc, G., Toczek, J., & Jaśkowski, W. (2016). ViZDoom: A doom-based AI research platform for visual reinforcement learning. *IEEE conference on computational intelligence and games*, 341–348. <https://doi.org/10.1109/CIG.2016.7860433>
- Kingma, D. P., & Ba, J. (2015). Adam: A method for stochastic optimization. In Y. Bengio & Y. LeCun (Eds.), *3rd international conference on learning representations, ICLR 2015, san diego, CA, USA, may 7-9, 2015, conference track proceedings*. <https://doi.org/10.48550/arXiv.1412.6980>
- LeCun, Y., Bengio, Y., & Hinton, G. (2015). Deep learning [Number: 7553 Publisher: Nature Publishing Group]. *Nature*, *521*(7553), 436–444. <https://doi.org/10.1038/nature14539>
- Mnih, V., Badia, A. P., Mirza, M., Graves, A., Lillicrap, T., Harley, T., Silver, D., & Kavukcuoglu, K. (2016). Asynchronous methods for deep reinforcement learning [ISSN: 1938-7228]. *Proceedings of The 33rd International Conference on Machine Learning*, 1928–1937. Retrieved June 1, 2023, from <https://proceedings.mlr.press/v48/mniha16.html>

- Mnih, V., Kavukcuoglu, K., Silver, D., Graves, A., Antonoglou, I., Wierstra, D., & Riedmiller, M. (2013, December 19). Playing atari with deep reinforcement learning. <https://doi.org/10.48550/arXiv.1312.5602>
- Mnih, V., Kavukcuoglu, K., Silver, D., Rusu, A. A., Veness, J., Bellemare, M. G., Graves, A., Riedmiller, M., Fidjeland, A. K., Ostrovski, G., Petersen, S., Beattie, C., Sadik, A., Antonoglou, I., King, H., Kumaran, D., Wierstra, D., Legg, S., & Hassabis, D. (2015). Human-level control through deep reinforcement learning [Number: 7540 Publisher: Nature Publishing Group]. *Nature*, *518*(7540), 529–533. <https://doi.org/10.1038/nature14236>
- OpenAI. (2023, March 27). GPT-4 technical report. <https://doi.org/10.48550/arXiv.2303.08774>
- OpenAI, Berner, C., Brockman, G., Chan, B., Cheung, V., Dębiak, P., Denison, C., Farhi, D., Fischer, Q., Hashme, S., Hesse, C., Józefowicz, R., Gray, S., Olsson, C., Pachocki, J., Petrov, M., Pinto, H. P. d. O., Raiman, J., Salimans, T., . . . Zhang, S. (2019, December 13). Dota 2 with large scale deep reinforcement learning. <https://doi.org/10.48550/arXiv.1912.06680>
- Paszke, A., Gross, S., Massa, F., Lerer, A., Bradbury, J., Chanan, G., Killeen, T., Lin, Z., Gimelshein, N., Antiga, L., Desmaison, A., Kopf, A., Yang, E., DeVito, Z., Raison, M., Tejani, A., Chilamkurthy, S., Steiner, B., Fang, L., . . . Chintala, S. (2019). PyTorch: An imperative style, high-performance deep learning library. *Advances in Neural Information Processing Systems*, *32*. Retrieved June 1, 2023, from <https://proceedings.neurips.cc/paper/2019/hash/bdbca288fee7f92f2bfa9f7012727740-Abstract.html>
- Pollack, J., & Blair, A. (1996). Why did TD-gammon work? *Advances in Neural Information Processing Systems*, *9*. Retrieved August 26, 2023, from https://papers.nips.cc/paper_files/paper/1996/hash/459a4ddcb586f24efd9395aa7662bc7c-Abstract.html
- Raffin, A., Hill, A., Gleave, A., Kanervisto, A., Ernestus, M., & Dormann, N. (2021). Stable-baselines3: Reliable reinforcement learning implementations. *Journal of Machine Learning Research*, *22*(268), 1–8. Retrieved June 1, 2023, from <http://jmlr.org/papers/v22/20-1364.html>
- Russell, S., & Norvig, P. (2020). *Artificial intelligence: A modern approach (4th edition)*. Pearson. Retrieved August 25, 2023, from <http://aima.cs.berkeley.edu/>
- Schaul, T., Quan, J., Antonoglou, I., & Silver, D. (2016, May 2). Prioritized experience replay. In Y. Bengio & Y. LeCun (Eds.), *4th international conference on learning representations, ICLR 2016 - conference track proceedings*. <http://arxiv.org/abs/1511.05952>

- Schrittwieser, J., Antonoglou, I., Hubert, T., Simonyan, K., Sifre, L., Schmitt, S., Guez, A., Lockhart, E., Hassabis, D., Graepel, T., Lillicrap, T., & Silver, D. (2020). Mastering atari, go, chess and shogi by planning with a learned model [Number: 7839 Publisher: Nature Publishing Group]. *Nature*, *588*(7839), 604–609. <https://doi.org/10.1038/s41586-020-03051-4>
- Schulman, J., Levine, S., Abbeel, P., Jordan, M., & Moritz, P. (2015). Trust region policy optimization [ISSN: 1938-7228]. *Proceedings of the 32nd International Conference on Machine Learning*, 1889–1897. Retrieved August 29, 2023, from <https://proceedings.mlr.press/v37/schulman15.html>
- Schulman, J., Wolski, F., Dhariwal, P., Radford, A., & Klimov, O. (2017, August 28). Proximal policy optimization algorithms. <https://doi.org/10.48550/arXiv.1707.06347>
- Senior, A. W., Evans, R., Jumper, J., Kirkpatrick, J., Sifre, L., Green, T., Qin, C., vZidek, A., Nelson, A. W. R., Bridgland, A., Penedones, H., Petersen, S., Simonyan, K., Crossan, S., Kohli, P., Jones, D. T., Silver, D., Kavukcuoglu, K., & Hassabis, D. (2020). Improved protein structure prediction using potentials from deep learning [Number: 7792 Publisher: Nature Publishing Group]. *Nature*, *577*(7792), 706–710. <https://doi.org/10.1038/s41586-019-1923-7>
- Silver, D. (2015). *Advanced topics in machine learning* [David silver]. Retrieved August 29, 2023, from <https://www.davidsilver.uk/teaching/>
- Silver, D., Huang, A., Maddison, C. J., Guez, A., Sifre, L., van den Driessche, G., Schrittwieser, J., Antonoglou, I., Panneershelvam, V., Lanctot, M., Dieleman, S., Grewe, D., Nham, J., Kalchbrenner, N., Sutskever, I., Lillicrap, T., Leach, M., Kavukcuoglu, K., Graepel, T., & Hassabis, D. (2016). Mastering the game of go with deep neural networks and tree search [Number: 7587 Publisher: Nature Publishing Group]. *Nature*, *529*(7587), 484–489. <https://doi.org/10.1038/nature16961>
- Silver, D., Hubert, T., Schrittwieser, J., Antonoglou, I., Lai, M., Guez, A., Lanctot, M., Sifre, L., Kumaran, D., Graepel, T., Lillicrap, T., Simonyan, K., & Hassabis, D. (2018). A general reinforcement learning algorithm that masters chess, shogi, and go through self-play [Publisher: American Association for the Advancement of Science]. *Science*, *362*(6419), 1140–1144. <https://doi.org/10.1126/science.aar6404>
- Silver, D., Schrittwieser, J., Simonyan, K., Antonoglou, I., Huang, A., Guez, A., Hubert, T., Baker, L., Lai, M., Bolton, A., Chen, Y., Lillicrap, T., Hui, F., Sifre, L., van den Driessche, G., Graepel, T., & Hassabis, D. (2017). Mastering the game of go without human knowledge [Number:

- 7676 Publisher: Nature Publishing Group]. *Nature*, 550(7676), 354–359. <https://doi.org/10.1038/nature24270>
- Song, H., Haustein, J. A., Yuan, W., Hang, K., Wang, M. Y., Kragic, D., & Stork, J. A. (2020). Multi-object rearrangement with monte carlo tree search: A case study on planar nonprehensile sorting [ISSN: 2153-0866]. *2020 IEEE/RSJ International Conference on Intelligent Robots and Systems (IROS)*, 9433–9440. <https://doi.org/10.1109/IROS45743.2020.9341532>
- Sutton, R. S. (1988). Learning to predict by the methods of temporal differences. *Machine Learning*, 3(1), 9–44. <https://doi.org/10.1007/BF00115009>
- Sutton, R. S., & Barto, A. G. (2018). *Reinforcement learning: An introduction* (Second edition). The MIT Press.
- Terry, J., Black, B., Grammel, N., Jayakumar, M., Hari, A., Sullivan, R., Santos, L. S., Dieffendahl, C., Horsch, C., Perez-Vicente, R., et al. (2021). Pettingzoo: Gym for multi-agent reinforcement learning. *Advances in Neural Information Processing Systems*, 34, 15032–15043.
- Tesauro, G. (1994). TD-gammon, a self-teaching backgammon program, achieves master-level play. *Neural Computation*, 6(2), 215–219. <https://doi.org/10.1162/neco.1994.6.2.215>
- Tesauro, G. (1995). Temporal difference learning and TD-gammon. *Communications of the ACM*, 38(3), 58–68. <https://doi.org/10.1145/203330.203343>
- Towers, M., Terry, J. K., Kwiatkowski, A., Balis, J. U., Cola, G., Deleu, T., Goulão, M., Kallinteris, A., KG, A., Krimmel, M., Perez-Vicente, R., Pierré, A., Schulhoff, S., Tai, J. J., Tan, A. J. S., & Younis, O. G. (2023, March). *Gymnasium*. Zenodo. <https://doi.org/10.5281/zenodo.8269265>
- Tsitsiklis, J., & Van Roy, B. (1997). An analysis of temporal-difference learning with function approximation [Conference Name: IEEE Transactions on Automatic Control]. *IEEE Transactions on Automatic Control*, 42(5), 674–690. <https://doi.org/10.1109/9.580874>
- van Hasselt, H., Guez, A., & Silver, D. (2016). Deep reinforcement learning with double q-learning [Number: 1]. *Proceedings of the AAAI Conference on Artificial Intelligence*, 30(1). <https://doi.org/10.1609/aaai.v30i1.10295>
- Watkins, C. J. C. H., & Dayan, P. (1992). Q-learning. *Machine Learning*, 8(3), 279–292. <https://doi.org/10.1007/BF00992698>
- Williams, R. J. (1992). Simple statistical gradient-following algorithms for connectionist reinforcement learning. *Machine Learning*, 8(3), 229–256. <https://doi.org/10.1007/BF00992696>

- Wu, Y., Mansimov, E., Grosse, R. B., Liao, S., & Ba, J. (2017). Scalable trust-region method for deep reinforcement learning using kronecker-factored approximation. *Advances in Neural Information Processing Systems*, 30. Retrieved September 2, 2023, from https://proceedings.neurips.cc/paper_files/paper/2017/hash/361440528766bbaaaa1901845cf4152b-Abstract.html
- Zeng, A., Song, S., Welker, S., Lee, J., Rodriguez, A., & Funkhouser, T. (2018). Learning synergies between pushing and grasping with self-supervised deep reinforcement learning. *IEEE International Conference on Intelligent Robots and Systems (IROS)*. <https://doi.org/10.1109/IROS.2018.8593986>
- Zhang, H., & Yu, T. (2020). Taxonomy of reinforcement learning algorithms. In H. Dong, Z. Ding, & S. Zhang (Eds.), *Deep reinforcement learning: Fundamentals, research and applications* (pp. 125–133). Springer. https://doi.org/10.1007/978-981-15-4095-0_3
- Zhong, M., Johnson, M., Tassa, Y., Erez, T., & Todorov, E. (2013). Value function approximation and model predictive control [ISSN: 2325-1867]. *2013 IEEE Symposium on Adaptive Dynamic Programming and Reinforcement Learning (ADPRL)*, 100–107. <https://doi.org/10.1109/ADPRL.2013.6614995>

List of Figures

1.1	Frames of different Atari games	2
1.2	International champion plays against AlphaGo	2
2.1	The agent-environment interaction in an MDP.	11
2.2	Backup diagrams for v_* and q_*	15
2.3	Taxonomy of RL algorithms.	17
3.1	Generalised Policy Iteration	21
5.1	BGE environment	45
5.2	Agent observation	47
5.3	Unsuccessful episode	48
5.4	Successful episode	48
5.5	Domain randomisation	51
5.6	Network architecture for DQN	54
5.7	Network architecture for PPO and A2C	55
6.1	Agent performance in experiment I.	61
6.2	Agent performance in experiment II.	63
6.3	Agent performance in experiment III.	65
6.4	Agent performance in experiment IV.	67
6.5	Agent performance in experiment V.	69
6.6	Agent performance in experiment VI.	72

List of Algorithms

1	SARSA(0), On-policy TD Control	25
2	Q-Learning, Off-policy TD Control	25
3	Semi-gradient SARSA(0), On-policy TD Control	28
4	Deep Q-Learning with Experience Replay	31
5	REINFORCE: Monte-Carlo Policy-Gradient Control	33
6	REINFORCE with Baseline	34
7	SARSA(0) Actor-Critic	36
8	(Synchronous) One-step Advantage Actor-Critic (A2C)	37
9	Proximal Policy Optimisation (Clip)	38
10	Example code for training an agent on BGE	56

List of Tables

5.1	DQN Hyperparameters	57
5.2	PPO Hyperparameters	57
5.3	A2C Hyperparameters	58
5.4	Description of environment parameters	58
6.1	Environment parameters for experiments	59
6.2	Environment parameters for experiment I	60
6.3	Baseline performance for experiment I	60
6.4	Final performance for experiment I	60
6.5	Environment parameters for experiment II	62
6.6	Baseline performance for experiment II	62
6.7	Final performance for experiment II	62
6.8	Environment parameters for experiment III	64
6.9	Baseline performance for experiment III	64
6.10	Final performance for experiment III	64
6.11	Environment parameters for experiment IV	66
6.12	Baseline performance for experiment IV	66
6.13	Final performance for experiment IV	66
6.14	Environment parameters for experiment V	68
6.15	Baseline performance for experiment V	68
6.16	Final performance for experiment V	68
6.17	Environment parameters for experiment VI	71
6.18	Baseline performance for experiment VI	71
6.19	Final performance for experiment VI	71

List of Acronyms

- A2C** Advantage Actor-Critic. i, ii, 6, 19, 36, 39, 54–56, 62, 64, 66, 70
A3C Asynchronous Advantage Actor-Critic. 36, 42
AAN Artificial Neural Network. 3, 7, 26
ALE Arcade Learning Environment. 3, 41, 42
BGE Bidimensional Gripper Environment. i, ii, 6, 45, 46, 56, 76, 87, 89
CNN Convolutional Neural Network. 3, 4, 41, 43, 52, 54, 55, 76, 77
DL Deep Learning. 1, 4, 5, 7
DNN Deep Neural Network. 4, 43, 53, 76
DP Dynamic Programming. 14, 20, 23, 24, 26
DQfD Deep Q-learning from Demonstrations. 41, 42
DQN Deep Q-Network. i, ii, 3, 6, 19, 20, 29–31, 41, 53, 54, 56, 62, 64, 66, 68, 70, 73, 76
DRL Deep Reinforcement Learning. i, ii, 1, 3–6, 12, 13, 29, 41–43, 76, 77
GPI Generalised Policy Iteration. 21–24, 26
MARL Multi-Agent Reinforcement Learning. 43
MC Monte Carlo. 23, 24, 27, 33, 34
MCTS Monte Carlo Tree Search. 4, 44
MDP Markov Decision Process. 7–9, 11, 12, 20, 42, 43, 47, 87
MPC Model Predictive Control. 43
PPO Proximal Policy Optimisation. i, ii, 4, 6, 19, 37–39, 42, 54–56, 62, 64, 66, 70, 73
RL Reinforcement Learning. i, ii, 1–8, 10, 13–19, 21–27, 41–43, 45, 49, 77, 87
SARSA State–action–reward–state–action. 24, 25, 28, 29, 35, 36, 89
SGD Stochastic Gradient Descent. 27, 39
SL Supervised Learning. 1, 4
TD Temporal Difference. 3, 24–27, 30, 31, 35, 36, 42

Appendix A

Summary of Notation

Capital letters are used for random variables, whereas lower case letters are used for the values of random variables and for scalar functions. Quantities that are required to be real-valued vectors are written in bold and in lower case (even if random variables). Matrices are bold capitals.

\doteq	equality relationship that is true by definition
\approx	approximately equal
\propto	proportional to
$\Pr\{X=x\}$	probability that a random variable X takes on the value x
$X \sim p$	random variable X selected from distribution $p(x) \doteq \Pr\{X=x\}$
$\mathbb{E}[X]$	expectation of a random variable X , i.e., $\mathbb{E}[X] \doteq \sum_x p(x)x$
$\arg \max_a f(a)$	a value of a at which $f(a)$ takes its maximal value
$\ln x$	natural logarithm of x
e^x	the base of the natural logarithm, $e \approx 2.71828$, carried to power x ; $e^{\ln x} = x$
\mathbb{R}	set of real numbers
$f : \mathcal{X} \rightarrow \mathcal{Y}$	function f from elements of set \mathcal{X} to elements of set \mathcal{Y}
\leftarrow	assignment
$(a, b]$	the real interval between a and b including b but not including a
ε	probability of taking a random action in an ε -greedy policy
α, β	step-size parameters
γ	discount-rate parameter
λ	decay-rate parameter for eligibility traces
$\mathbb{1}_{predicate}$	indicator function ($\mathbb{1}_{predicate} \doteq 1$ if the <i>predicate</i> is true, else 0)

In a Markov Decision Process:

s, s'	states
a	an action
r	a reward
\mathcal{S}	set of all nonterminal states
\mathcal{S}^+	set of all states, including the terminal state
$\mathcal{A}(s)$	set of all actions available in state s
\mathcal{R}	set of all possible rewards, a finite subset of \mathbb{R}

\subset	subset of; e.g., $\mathcal{R} \subset \mathbb{R}$
\in	is an element of; e.g., $s \in \mathcal{S}$, $r \in \mathcal{R}$
$ \mathcal{S} $	number of elements in set \mathcal{S}
t	discrete time step
$T, T(t)$	final time step of an episode, or of the episode including time step t
A_t	action at time t
S_t	state at time t , typically due, stochastically, to S_{t-1} and A_{t-1}
R_t	reward at time t , typically due, stochastically, to S_{t-1} and A_{t-1}
π	policy (decision-making rule)
$\pi(s)$	action taken in state s under <i>deterministic</i> policy π
$\pi(a s)$	probability of taking action a in state s under <i>stochastic</i> policy π
G_t	return following time t
h	horizon, the time step one looks up to in a forward view
$G_{t:t+n}, G_{t:h}$	n -step return from $t+1$ to $t+n$, or to h (discounted and corrected)
$\bar{G}_{t:h}$	flat return (undiscounted and uncorrected) from $t+1$ to h
G_t^λ	λ -return
$G_{t:h}^\lambda$	truncated, corrected λ -return
$G_t^{\lambda s}, G_t^{\lambda a}$	λ -return, corrected by estimated state, or action, values
$p(s', r s, a)$	probability of transition to state s' with reward r , from state s and action a
$p(s' s, a)$	probability of transition to state s' , from state s taking action a
$r(s, a)$	expected immediate reward from state s after action a
$r(s, a, s')$	expected immediate reward on transition from s to s' under action a
$v_\pi(s)$	value of state s under policy π (expected return)
$v_*(s)$	value of state s under the optimal policy
$q_\pi(s, a)$	value of taking action a in state s under policy π
$q_*(s, a)$	value of taking action a in state s under the optimal policy
V, V_t	array estimates of state-value function v_π or v_*
Q, Q_t	array estimates of action-value function q_π or q_*
$\bar{V}_t(s)$	expected approximate action value, e.g., $\bar{V}_t(s) \doteq \sum_a \pi(a s) Q_t(s, a)$
U_t	target for estimate at time t
δ_t	temporal-difference (TD) error at t (a random variable)
δ_t^s, δ_t^a	state- and action-specific forms of the TD error
n	in n -step methods, n is the number of steps of bootstrapping
d	dimensionality—the number of components of \mathbf{w}
d'	alternate dimensionality—the number of components of $\boldsymbol{\theta}$
\mathbf{w}, \mathbf{w}_t	d -vector of weights underlying an approximate value function
$w_i, w_{t,i}$	i th component of learnable weight vector
$\hat{v}(s, \mathbf{w})$	approximate value of state s given weight vector \mathbf{w}
$v_{\mathbf{w}}(s)$	alternate notation for $\hat{v}(s, \mathbf{w})$
$\hat{q}(s, a, \mathbf{w})$	approximate value of state-action pair s, a given weight vector \mathbf{w}
$\nabla \hat{v}(s, \mathbf{w})$	column vector of partial derivatives of $\hat{v}(s, \mathbf{w})$ with respect to \mathbf{w}
$\nabla \hat{q}(s, a, \mathbf{w})$	column vector of partial derivatives of $\hat{q}(s, a, \mathbf{w})$ with respect to \mathbf{w}

$\mathbf{x}(s)$	vector of features visible when in state s
$\mathbf{x}(s, a)$	vector of features visible when in state s taking action a
$x_i(s), x_i(s, a)$	i th component of vector $\mathbf{x}(s)$ or $\mathbf{x}(s, a)$
\mathbf{x}_t	shorthand for $\mathbf{x}(S_t)$ or $\mathbf{x}(S_t, A_t)$
$\mathbf{w}^\top \mathbf{x}$	inner product of vectors, $\mathbf{w}^\top \mathbf{x} \doteq \sum_i w_i x_i$; e.g., $\hat{v}(s, \mathbf{w}) \doteq \mathbf{w}^\top \mathbf{x}(s)$
\mathbf{v}, \mathbf{v}_t	secondary d -vector of weights, used to learn \mathbf{w}
\mathbf{z}_t	d -vector of eligibility traces at time t
$\boldsymbol{\theta}, \boldsymbol{\theta}_t$	parameter vector of target policy
$\pi(a s, \boldsymbol{\theta})$	probability of taking action a in state s given parameter vector $\boldsymbol{\theta}$
$\pi_{\boldsymbol{\theta}}$	policy corresponding to parameter $\boldsymbol{\theta}$
$\nabla \pi(a s, \boldsymbol{\theta})$	column vector of partial derivatives of $\pi(a s, \boldsymbol{\theta})$ with respect to $\boldsymbol{\theta}$
$J(\boldsymbol{\theta})$	performance measure for the policy $\pi_{\boldsymbol{\theta}}$
$\nabla J(\boldsymbol{\theta})$	column vector of partial derivatives of $J(\boldsymbol{\theta})$ with respect to $\boldsymbol{\theta}$
$h(s, a, \boldsymbol{\theta})$	preference for selecting action a in state s based on $\boldsymbol{\theta}$
$b(a s)$	behavior policy used to select actions while learning about target policy π
$b(s)$	a baseline function $b : \mathcal{S} \mapsto \mathbb{R}$ for policy-gradient methods
b	branching factor for an MDP or search tree
$\rho_{t:h}$	importance sampling ratio for time t through time h
ρ_t	importance sampling ratio for time t alone, $\rho_t \doteq \rho_{t:t}$
$r(\pi)$	average reward (reward rate) for policy π
\bar{R}_t	estimate of $r(\pi)$ at time t
$\mu(s)$	on-policy distribution over states
$\boldsymbol{\mu}$	$ \mathcal{S} $ -vector of the $\mu(s)$ for all $s \in \mathcal{S}$
$\ v\ _\mu^2$	μ -weighted squared norm of value function v , i.e., $\ v\ _\mu^2 \doteq \sum_{s \in \mathcal{S}} \mu(s) v(s)^2$
$\eta(s)$	expected number of visits to state s per episode
Π	projection operator for value functions
B_π	Bellman operator for value functions
\mathbf{A}	$d \times d$ matrix $\mathbf{A} \doteq \mathbb{E} \left[\mathbf{x}_t (\mathbf{x}_t - \gamma \mathbf{x}_{t+1})^\top \right]$
\mathbf{b}	d -dimensional vector $\mathbf{b} \doteq \mathbb{E} [R_{t+1} \mathbf{x}_t]$
\mathbf{w}_{TD}	TD fixed point $\mathbf{w}_{\text{TD}} \doteq \mathbf{A}^{-1} \mathbf{b}$ (a d -vector)
\mathbf{I}	identity matrix
\mathbf{P}	$ \mathcal{S} \times \mathcal{S} $ matrix of state-transition probabilities under π
\mathbf{D}	$ \mathcal{S} \times \mathcal{S} $ diagonal matrix with $\boldsymbol{\mu}$ on its diagonal
\mathbf{X}	$ \mathcal{S} \times d$ matrix with the $\mathbf{x}(s)$ as its rows
$\bar{\delta}_{\mathbf{w}}(s)$	Bellman error (expected TD error) for $v_{\mathbf{w}}$ at state s
$\bar{\delta}_{\mathbf{w}}, \text{BE}$	Bellman error vector, with components $\bar{\delta}_{\mathbf{w}}(s)$
$\overline{\text{VE}}(\mathbf{w})$	mean square value error $\overline{\text{VE}}(\mathbf{w}) \doteq \ v_{\mathbf{w}} - v_\pi\ _\mu^2$
$\overline{\text{BE}}(\mathbf{w})$	mean square Bellman error $\overline{\text{BE}}(\mathbf{w}) \doteq \ \bar{\delta}_{\mathbf{w}}\ _\mu^2$
$\overline{\text{PBE}}(\mathbf{w})$	mean square projected Bellman error $\overline{\text{PBE}}(\mathbf{w}) \doteq \ \Pi \bar{\delta}_{\mathbf{w}}\ _\mu^2$
$\overline{\text{TDE}}(\mathbf{w})$	mean square temporal-difference error $\overline{\text{TDE}}(\mathbf{w}) \doteq \mathbb{E}_b [\rho_t \delta_t^2]$
$\overline{\text{RE}}(\mathbf{w})$	mean square return error

